NATURAL RESOURCES

# Geologic Map of the Utsalady and Conway 7.5-minute Quadrangles, Skagit, Snohomish, and Island Counties, Washington

by Joe D. Dragovich,
Lea A. Gilbertson,
David K. Norman,
Garth Anderson,
and Gary T. Petro

WASHINGTON
DIVISION OF GEOLOGY
AND EARTH RESOURCES

Open File Report 2002-5
October 2002
Revised July 2004

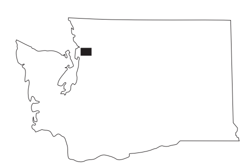

map location

WASHINGTON STATE DEPARTMENT OF
**Natural Resources**
**Doug Sutherland** - Commissioner of Public Lands

# Geologic Map of the Utsalady and Conway 7.5-minute Quadrangles, Skagit, Snohomish, and Island Counties, Washington

by Joe D. Dragovich,
Lea A. Gilbertson,
David K. Norman,
Garth Anderson,
and Gary T. Petro

WASHINGTON
DIVISION OF GEOLOGY
AND EARTH RESOURCES

Open File Report 2002-5
October 2002

Revised July 2004

*Produced in cooperation with the U.S. Geological Survey*
*National Cooperative Geologic Mapping Program*
*Agreement Number 00HQAG0107*

WASHINGTON STATE DEPARTMENT OF
**Natural Resources**
**Doug Sutherland** - Commissioner of Public Lands

## DISCLAIMER



**WASHINGTON DEPARTMENT OF NATURAL RESOURCES**

Doug Sutherland—*Commissioner of Public Lands*

**DIVISION OF GEOLOGY AND EARTH RESOURCES**

Ron Teissere—*State Geologist*
David K. Norman—*Assistant State Geologist*

Washington Department of Natural Resources
Division of Geology and Earth Resources
PO Box 47007
Olympia, WA 98504-7007
*Phone:* 360-902-1450
*Fax:* 360-902-1785
*E-mail:* geology@wadnr.gov
*Website:* http://www.dnr.wa.gov/geology/

Published in the United States of America

# Contents



## APPENDICES



## FIGURES



## PLATES

# Geologic Map of the Utsalady and Conway 7.5-minute Quadrangles, Skagit, Snohomish, and Island Counties, Washington

Joe D. Dragovich, Lea A. Gilbertson, David K. Norman, Garth Anderson, and Gary T. Petro
Washington Division of Geology and Earth Resources
PO Box 47007; Olympia, WA 98504-7007
joe.dragovich@wadnr.gov

## INTRODUCTION

The Utsalady and Conway 7.5-minute quadrangles are located in the northeastern portion of the Puget Lowland (Fig. 1). We group the geologic units in this area into: (1) Holocene alluvium, lahar runout, nearshore, beach, and landslide deposits; (2) Pleistocene glacial and nonglacial deposits; (3) Tertiary sedimentary and volcanic bedrock; and (4) Mesozoic metamorphic bedrock (Fig. 2).

Long-term movement along the Darrington–Devils Mountain fault zone (Tabor, 1994) has tectonically juxtaposed the Helena–Haystack mélange, Chuckanut Formation, and rocks of Bulson Creek in the northeastern portion of the study area. This regional fault zone may still be active (Johnson and others, 2001).

Late Pleistocene (Fraser age) glacial deposits mantle the mountains, foothills, and hills of the study area. Advance of the Puget lobe during the Vashon Stade of the last glaciation resulted in deposition of till over much of the area. Subglacial meltwater excavated the Skagit River valley (Booth, 1987, 1994). During the Everson Interstade, the lobe wasted back through the northern half of the Puget Lowland as marine waters entered the depressed Puget Sound basin and buoyed up the rapidly retreating and thinning ice. Marine and estuarine conditions then prevailed in the study area, producing a blanket of glaciomarine drift that is now at an elevation of 350 to 400 ft (107–122 m) as a result of isostatic rebound. Interfingering marine, estuarine, deltaic, and fluvial deposits of Everson age indicate a complex mix of depositional environments during that time. Facies vary vertically and horizontally from fine distal marine to coarse proximal outwash. Field mapping and subsurface analysis of Quaternary deposits indicate that pre-Fraser glacial and nonglacial deposits commonly underlie Vashon till and advance outwash and (or) glacial lake deposits and Everson recessional glacial deposits at shallow depths.

Sediment from Glacier Peak volcano was deposited in the study area via two routes (Fig. 1). Along one route, the White Chuck volcanic assemblage of Beget (1981, 1982) was deposited at the same time as Everson Interstade glacial outwash. We have found probable White Chuck assemblage dacite clasts in late-glacial outwash in the southeastern Conway quadrangle. This outwash appears to be restricted to near the intersection of the Stillaguamish River and the Puget Lowland. The outwash probably traveled down the Stillaguamish River and formed an outwash apron on the glacial uplands. Along the second route, dacite-rich volcanic sands form the uppermost Skagit Valley fill in the north-central Conway quadrangle. We interpreted these as lahar runout sands that traveled down the Skagit River and were deposited on or near the Skagit River delta about 1,700 to 1,800 yr B.P.

## METHODS, PREVIOUS WORK, RELATED STUDIES AND UNPUBLISHED DATA

Our mapping is based on field work completed in 2000 and 2001. We supplemented our field mapping with photo analysis of 1995–96 Washington State Department of Natural Resources (DNR) black and white ~1:13,000-scale aerial photos, 1993 and 1998 DNR 1:12,000-scale orthophotos, and 1942 U.S. Army 1:20,000-scale aerial photos. We petrographically analyzed 58 thin sections of Eocene volcanic and pre-Tertiary rocks from inside and outside the study area. Thin sections were prepared for point count studies of sedimentary rocks and unconsolidated sediments to determine lithologic character and sediment source(s). We also compiled data from 525 water well logs and 60 geotechnical boring logs in and adjacent to the Utsalady and Conway quadrangles. We ranked water-well logs according to quality of material descriptions and overall correspondence to nearby mapped outcrops. These logs were used to construct

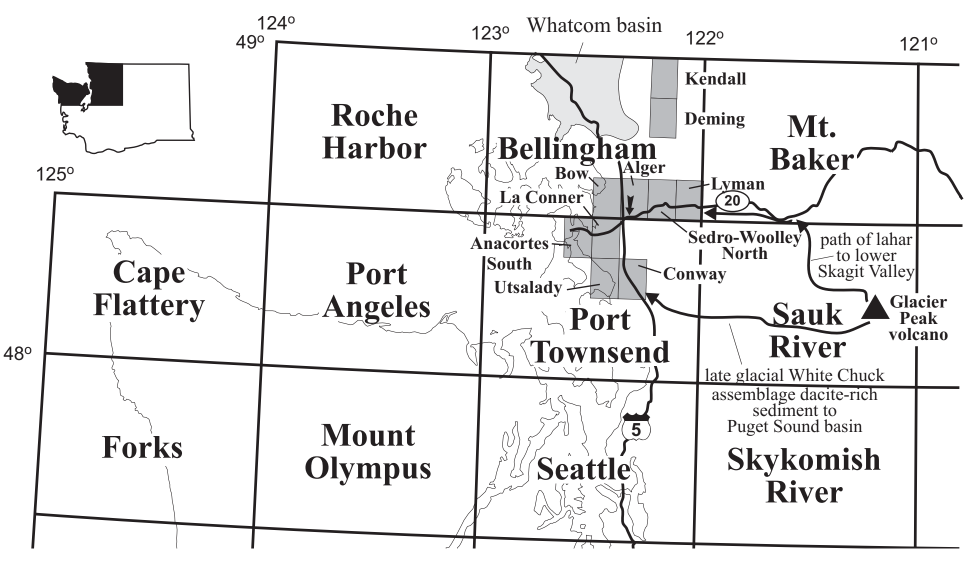


**Figure 1.** Location of 1:100,000-scale quadrangles and past and current STATEMAP 7.5-minute mapping projects (darker pattern), northwestern Washington. Long arrows show the path of Glacier Peak lahars and lahar runout to the lower Skagit River valley.

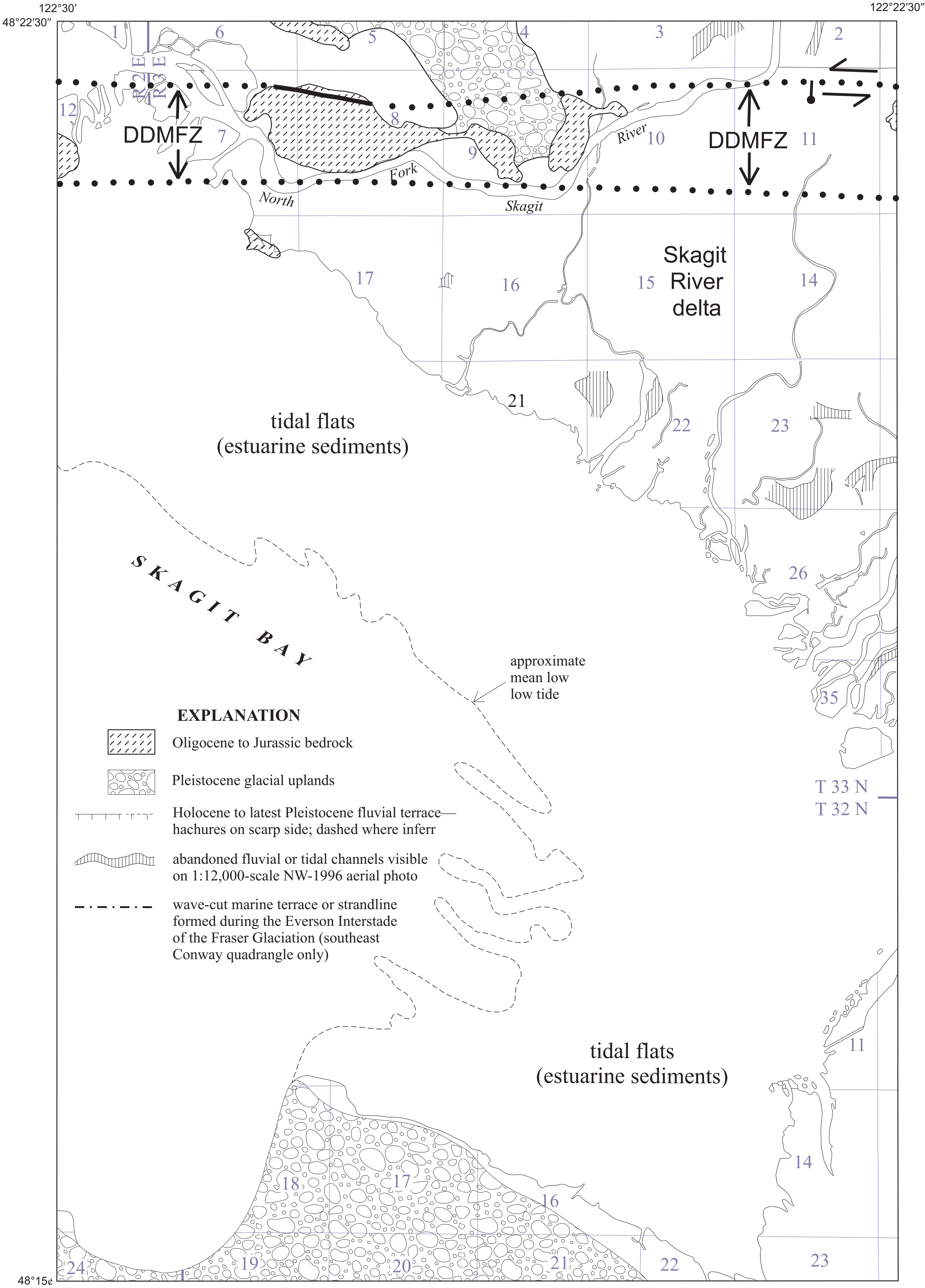


**Figure 2.** Generalized geologic provinces, abandoned channels, and terraces of the Utsalady *(this page)* and Conway *(facing page)* quadrangles. Provinces include Oligocene to Jurassic bedrock, Pleistocene glacial uplands, and Holocene Skagit River valley fill. Figure also shows the one

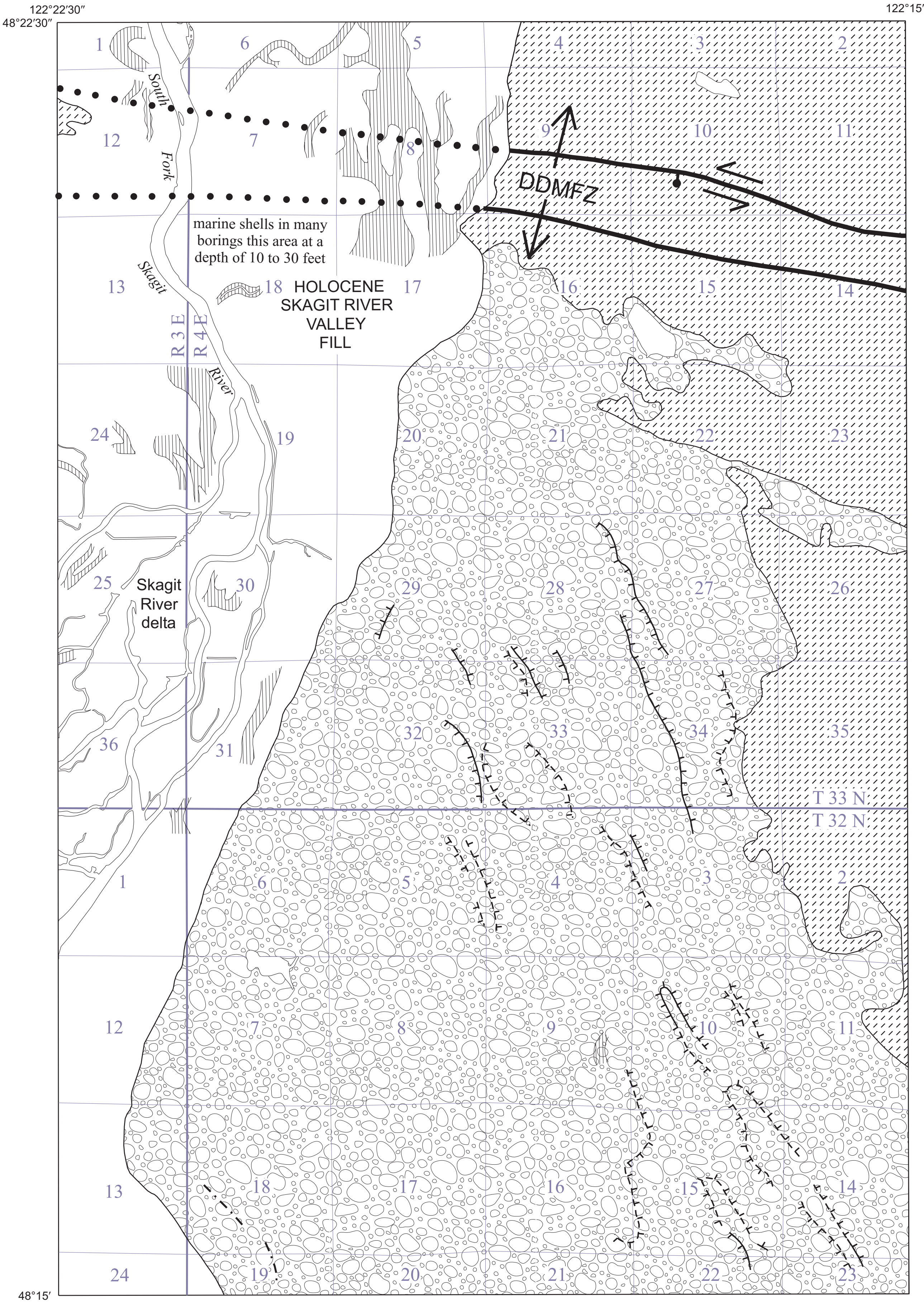


strandline in the southwestern portion of the Conway quadrangle interpreted using aerial photographs.

cross sections (Plate 2) and a map showing the inferred elevation of the surface of bedrock (Fig. 7).

Several previous studies in and adjacent to the study area contributed to our mapping and interpretations. These studies were Marcus (1981), Graham (1988), Whetten and others (1988), Pessl and others (1989), Johnson and others (2001), and Dethier and Safioles (1983).

## DESCRIPTIONS OF MAP UNITS

Each major lithostratigraphic unit in the study area is assigned a geologic symbol. Unit symbols provide information about the age, lithology, and name (if any) of the units: uppercase letters indicate protolith age, lowercase letters indicate lithology, and subscripts identify named units. For example, the Jurassic Helena–Haystack mélange metavolcanic rocks are shown with the symbol $Jmv_h$. We used the geologic time scale devised for the Correlation of Stratigraphic Units of North America (COSUNA) project of the American Association of Petroleum Geologists (Salvador, 1985). Extrusive volcanic rocks are categorized using various major-element geochemical classification schemes (Zanettin, 1984; Le Bas and others, 1986). Sandstones are named using the classification scheme of Folk (1980) or Dickinson (1970). Low-grade metamorphic rocks, including blueschist-facies rocks of the Helena–Haystack mélange, are described as metasedimentary or metavolcanic rocks. Landslides are classified using the terminology of Varnes (1978). We have not assigned stratigraphic thicknesses to most geologic units in the study area. See Marcus (1981) or Dragovich and Grisamer (1998) for additional information on the stratigraphic thicknesses of the geologic units in or around the study area.

### Quaternary Sedimentary and Volcanic Deposits

#### HOLOCENE NONGLACIAL DEPOSITS

Sediments of the Skagit River delta cover much of the study area. Late Holocene Skagit River delta progradation and associated fluvial vertical-accretion deposits of the present and ancient Skagit River have filled the former marine embayment of the lower Skagit River basin with approximately 200 to 400 ft (60–120 m) of unconsolidated Holocene sediment. Normal Skagit River delta sedimentation has been punctuated by voluminous input of lahar runout and volcanic alluvium from Holocene Glacier Peak eruptions (Dragovich and others 2000a,b, unpub. data). This valley-filling process has isolated several bedrock and glacial hills in the study area (Fig. 2).

The Skagit River delta includes both vertically and horizontally varying fluvial and deltaic facies and subfacies. We have mapped several geologic units separately in the Skagit River delta but acknowledge that many facies are gradational and difficult to map with confidence. Many contacts are inferred on the basis of aerial photographs, nearby field observations, or soil parent material information (Debose and Klungland, 1983; Klungland and McArthur, 1989). Skagit River delta stratigraphic information obtained from water-well and geotechnical-boring logs, as well as field observations, shows that alluvium commonly contains 20- to 40-ft (6–12 m) -thick sequences that generally fine upward from sandy channel deposits to silty overbank deposits. These sequences are probably the result of lateral migration of point bars, channel splays, or levees. These fluvial and deltaic deposits are locally capped by estuarine deposits and commonly overlie shell-bearing estuarine sediments that indicate earlier tide-dominated Skagit River delta fronts. In the northeastern portion of the Utsalady quadrangle and the northwestern portion of the Conway quadrangle, for example, sediments contain shells at a depth of 10 to 40 ft (3–12 m) across much of the present Skagit River delta top region, which indicates that the former Skagit River delta front occurs at a shallow depth (this study; Dragovich and others, 2000c).

Abandoned channels in the Skagit River valley (Fig. 2) appear as distinct to faint traces on aerial photos. These channels are commonly associated with arcuate lateral-accretion surfaces formed along ancestral Skagit River meander bends (Dragovich and others, 1999). Some of the abandoned channels are filled with lacustrine or peat deposits and form sinuous depressions 3 to 6 ft (1–2 m) deep. Historic dike building (Plate 1, unit af) has isolated many tidal channels from Puget Sound.

Paleogeography suggests that the Skagit River delta front was near Mount Vernon, significantly north of the study area, at about 5,000 yr B.P. and has prograded downvalley during the latter half of the Holocene (Thompson, 1978; Dragovich and others, 2000c). In the study area, most or all of the of the topset beds of the Skagit River delta were probably deposited in the last 2,000 years, as evidenced by radiocarbon ages obtained from peats, paleosols, organic mats, and human settlements (Thompson, 1978; this study).

Qb **Beach deposits (Holocene)—**Loose, moderately to well-sorted and well-rounded sand and gravel along modern shorelines; locally includes wave-worn shell fragments. The contact between beach and estuarine deposits (unit Qn) is typically gradational to locally sharp. Beach deposits are arbitrarily mapped to present sea level except where the transition from beach sand and gravel to silty tidal flat deposits is well exposed and sharp.

Qn **Nearshore deposits (Holocene)**—Estuarine or tidal flat deposits composed of loose or soft, gray to olive gray, fine to very fine sand, silty very fine sand, silt, silty clay, and bluish gray clay with various admixtures of organic material; logs occur locally; surficial stratum is commonly brown and (or) mottled brown or reddish brown to gray; organic strata commonly contain organic mats, lenses, and distinct layers from 1 to 3 in. (2–8 cm) thick; lesser medium to coarse sand occurs near fluvially influenced channels or abandoned channels; mostly massive to thinly bedded and locally micaceous.

Unit Qn includes both the present tidal flats, which are mostly devoid of vegetation or contain spotty mats of organic material about 1 in. thick (Klungland and McArthur, 1989), and older estuarine deposits northeast of the present Skagit River delta front. Upvalley areas may locally include a veneer of flood overbank deposits (unit $Qa_s$) and marsh or peat deposits (units Qm and Qp, respectively). The uppermost few feet of the Skagit Valley fill is typically structureless silt, massive (probably bioturbated) and more than 1 to 2 m thick. Fluvial overbank deposits commonly form thinly to very thinly bedded sequences of silt and fine sand as the result of repeated, vertically accreting flood deposits. We map most of the younger alluvium of Pessl and others (1989) as unit Qn.

Qm **Marsh deposits (Holocene)**—Mostly soft to stiff olive gray silt and silty clay, commonly with lenses and layers of peat, muck, and other organic material; locally contains 5-in. (~12 cm) -thick white or creamcolored layers of ash. Deposits occur above highest high tide and are covered with salt-tolerant vegetation. The contacts between marsh, Skagit River fluvial, and tidal flat environments are commonly gradational or masked by agricultural modifications, and thus contacts on Plate 1 are generally inferred.

$Qa_s$, $Qa_{sl}$ **Skagit River alluvium (Holocene)**—Active or abandoned channel and flood overbank deposits (unit $Qa_s$). Channel deposits are typically coarse grained and consist of loose gravelly sand and sand; mostly thin- to thick-bedded and plane-laminated. Clasts are subangular to subrounded and derived from volcanic, metamorphic, and plutonic bedrock in the upper part of the Skagit drainage and reworked lahar and glacial deposits. Sands are black or brown to gray, depending on oxidation state and composition, but typically are olive gray and have a 'salt and pepper' appearance resulting from the mixture of dark lithic clasts and opaque minerals with light-colored quartz, feldspar, and intermediate volcanic lithic clasts. Mica (1–3%) is conspicuous in the sands. Overbank deposits consist mostly of soft to stiff, grayish brown to olive gray stratified sand, fine sandy silt, silt, and silty clay with minor peat. Unit $Qa_s$ is locally divided into flood-plain splay deposits (unit $Qa_{sl}$). These splays are composed of sand and fine gravelly sand and form subtle to distinct levees adjacent to or near the present Skagit River channels.

Qp **Peat (Holocene)**—Mostly poorly stratified to unstratified, brown to black, soft fibrous to woody peat and muck of bogs and swamps of abandoned channels, kettles, and shallow oxbow lakes or other depressions; may contain volcanic ash. Not shown on Plate 1 are isolated peaty or marshy intertidal deposits associated with estuarine sediments (unit Qn) and other locally organic-rich areas found in the Skagit River valley alluvium as small oxbow lakes or depressions associated with abandoned channels.

Qaf **Alluvial fan deposits (Holocene to latest Pleistocene)**—Poorly sorted, massive to weakly stratified, soft to stiff, clayey silty sandy gravel and gravelly sandy silt with angular to rounded clasts; mostly of debris-flow or debris-torrent origin, locally modified by stream processes; clasts locally derived. Alluvial fans mostly overlie glacial deposits. Unit Qaf interfingers with alluvium and is mostly Holocene.

Qls **Landslide deposits (Holocene to latest Pleistocene)**—Mostly poorly sorted, unstratified, cohesive diamicton consisting of angular to rounded boulders, cobbles, and gravel in a soft sand, silt, and (or) clay matrix; contains clasts of local origin. Unit Qls includes deep-seated failures (slump-earthflow, debris slump, or rock slump) and rare rock avalanche, fall, topple, and slab failures. Younger, smaller, shallow slides are locally associated with deep-seated landslides. Although unit thickness varies greatly, deep-seated landslide deposits are typically about 30 ft (9 m) thick.

Landslides unconformably overlie bedrock, late glacial deposits, and other Quaternary geologic units and are thus mostly Holocene. However, the probability that unvegetated and locally steep slopes of unconsolidated glacial deposits were exposed during the Everson deglaciation suggests that some landslides are of late Pleistocene age and may interfinger with late glacial materials at depth. Some mass wastage may have been seismically induced.

Coastal bluffs of the Puget Sound are inherently unstable due to the generally poor consolidation and (or) low shear strength of the bluff strata. Also, wave action, longshore transport, and other agents tend to erode and destabilize the toes of bluffs. Pistol-butted trees, small rotated slump blocks, intense seepage, truncated Quaternary stratigraphic sequences, and other indicators of slope instability are present along many of the steeper coastal bluffs of the study area (such as Utsalady Point). However, many coastal areas lack distinct landslide morphology (for example, prominent flanks, toe, scarps, and main body). We have mapped only the most conspicuous coastal bluff landslides in the study area. (See also Keuler, 1988; Frederick, 1979; and a series of 1:24,000-scale maps, including slope stability hazard zonation maps, by the Washington Department of Ecology, 1978. Useful bluff slope stabilization and erosion control guides are also available from the Washington Department of Ecology [Myers Biodynamics, Inc., 1993; Myers Biodynamics, Inc., and Lorilla Engineering, Inc., 1995].)

Qvl **Lahar runout deposits (Holocene)**—Loose, well-sorted, medium to fine, light gray volcanic sand; subangular to subrounded; massive, may be normally graded. Lahar deposits are locally overlain by 0.1 to 2 ft (3–60 cm) of alluvial flood silt. We interpret unit Qvl as a hyperconcentrated flood or lahar runout deposit, using the terminology of Pierson and Scott (1985).

This sandy lahar is texturally and compositionally similar to the mid-Holocene noncohesive lahar of the Kennedy Creek assemblage north of the study area (Fig. 3), differing only in valley position and overall sand composition (Dragovich and others, 2000a,c, unpub. data). We have obtained radiocarbon ages of ~1,700 to 1,800 yr B.P. from this assemblage near Darrington (Dragovich and others, unpub. data) and tentatively correlate unit Qvl with the lahar near Burlington (Beget, 1981, 1982; Dethier and Whetten, 1981) and with the Chocolate Creek assemblage near Glacier Peak (Beget, 1981)(Fig. 3). We suggest that this lahar followed an ancestral Skagit River channel to the delta front, forming a small depositional lobe in the study area (this study; Dragovich and others, 2000c).

## PLEISTOCENE GLACIAL AND NONGLACIAL DEPOSITS

Armstrong and others (1965) divided the deposits of the Fraser Glaciation into those of the Sumas Stade, Everson Interstade, and Vashon Stade. Deposits of the Olympia nonglacial interval of Mullineaux and others (1965) and Armstrong and others (1965) represent the preceding interglaciation. Deposits of the Everson Interstade, Vashon Stade, and Olympia nonglacial interval are mapped in the study area (Plates 1 and 2). Older glacial and nonglacial deposits are inferred from subsurface information (Figs. 4 and 5; Plate 2, cross sections D–J).

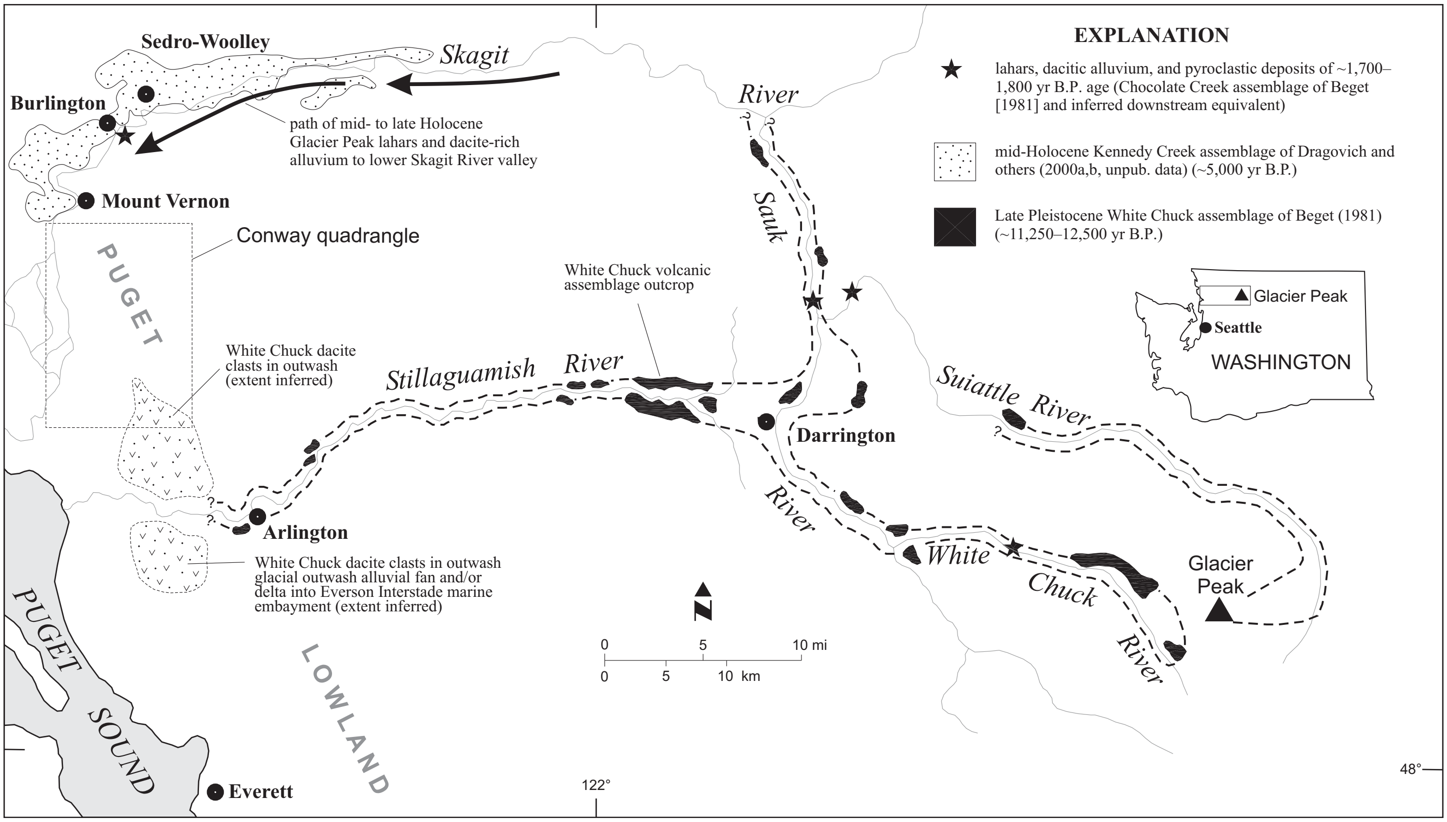


**Figure 3.** General location of distal Glacier Peak detritus and dacite-bearing outwash near the Conway 7.5-minute quadrangle. White Chuck volcanic assemblage (WCA) distribution modified after Beget (1982). Lower Skagit Valley Kennedy Creek assemblage (KCA) modified from Dragovich and others (2000a,c). Chocolate Creek assemblage dating sites (1,700–1,800 yr B.P.) from Beget (1981), Dethier and Whetten (1981), and Dragovich and others (unpub. data). Unit Qvl in the Conway quadrangle may be lahar runout from the late Holocene Chocolate Creek assemblage volcanic event. Foreset bedding and imbrications in recessional outwash in the southeastern portion of the Conway quadrangle indicate paleoflow to the west-northwest to northwest or from the ancient Stillaguamish into the Puget Lowland marine environment. Glacier Peak detritus was also transported to the study area as distinctive dacite clasts in recessional outwash (Appendix 4) and probably contains late-glacial WCA clasts. WCA pyroclastic flows comprise most of the WCA near the volcano where the assemblage is more than 320 ft (~100 m) thick, but beyond about 12 mi (~20 km) downstream, the assemblage consists entirely of volcanic alluvium and lahars. Glacier Peak lahars correlated with the late Pleistocene WCA are exposed 2 mi (~3 km) west of Arlington in the Stillaguamish Valley, more than 60 mi (~100 km) downstream from Glacier Peak. Our mapping supports the contention of Dethier and others (1995) that rivers and recessional meltwater evidently transported substantial sediment to glaciomarine settings. The Stillaguamish River likely had exceptional loads during the Everson Interstade as a result of catastrophic input of Glacier Peak volcaniclastic sediment to the White Chuck and Stillaguamish Rivers during ice retreat. The lahars near Arlington contain more than 95 percent dacite-rich volcanic debris that is only slightly vesicular and is similar to the dacite clasts in outwash of the study area. We have stylized the location of glacial outwash to show it as a sediment fan or delta at the intersection of the Puget Lowland with the Stillaguamish River. The late glacial alluvial fan–deltaic complex emanating from the ancient Stillaguamish River occurred near maximum glaciomarine inundation (~340 ft or ~105 m).

## Deposits of the Fraser Glaciation

### *Everson Interstade*

The period of ablation and recession of the Puget lobe during the Fraser Glaciation is termed the Everson Interstade. Paleogeography exerted major control on glacial-recessional depositional environments in the Skagit River valley (Dragovich and others, 1998, 1999, 2000b,c; Dethier and others, 1995). Complex facies relations occur at the interface between bedrock highlands and marine embayments. Everson sediments generally thicken and coarsen near ancient river and meltwater pathways leading to highland areas. The glacial uplands are mantled with terrestrial outwash (unit $Qgo_e$) above the glaciomarine limit; the outwash merges with glaciomarine deposits west of the highlands (Plate 2, cross section I). For example, in cross section D, well 410, and cross section E, well 165, thick outwash beds interfinger with glaciomarine diamicton and clay, indicating transitional facies conditions. Very thick Everson glaciomarine sections are common in the study area, particularly near bedrock uplands. They reflect high sedimentation rates in localized depocenters during deglaciation. Geochemical analyses, sand point-counts, dacite clast petrographic information, and field relations indicate that outwash containing significant Glacier Peak dacite detritus was deposited concurrently with glaciomarine drift in southern portion of the Conway quadrangle.

Composite Everson thicknesses range from a few feet to 250 ft (76 m). Deposits are typically 20 to 100 ft (6–31 m)(Plate 2, cross sections D–J). Dethier and others (1995, 1996) and Dragovich and others (for example, 2000b,c) map estuarine silt deposits that generally lack dropstones, locally exceed 60 ft (18 m) thick (Plate 2, cross section E, well 482), and define the uppermost part of an overall upward-fining Everson glaciomarine stratigraphic sequence common in the lower Skagit River valley. (See also Dragovich and others, 1998, 2000b; Dragovich and Grisamer, 1998.) Conversely, outwash deltaic progradation into the former lower Skagit marine embayment resulted locally in an overall upward-coarsening sequence from open glaciomarine to deltaic depositional environments. (For additional information on Everson sedimentary facies analyses, paleoecology, and paleogeography, see Croll, 1980; Balzarini, 1981, 1983; Carlstad, 1992).

Radiocarbon ages for Everson glaciomarine deposits near the study area are consistent with local and regional ages of the Everson glaciomarine drift and related deposits of about 13,600 to 11,000 yr B.P. (Easterbrook, 1962, 1963a, 1992; Dragovich and others, 1998, 1999, 2000b,c, unpub. data; Armstrong and others, 1965; Dethier and others, 1995). Age relations indicate maximum Everson glaciomarine inundation or highest marine limit south of a stagnating ice front in the lower Skagit River valley before about 12,900 yr B.P. (Dragovich and others, 1998, 1999). Dragovich and others (1998) obtained a radiocarbon date of 13,270 ±50 yr B.P. from shell fragments in glaciomarine gravelly clay at an altitude of about 340 ft (104 m) along a logging road on Burlington Hill north of the study area. This age probably approximates the age of maximum glaciomarine inundation in the lower Skagit River valley. Dethier and others (1995) obtained a shell age of 11,300 ±79 yr B.P. from fossiliferous glaciomarine diamicton over outwash gravel in Dodge Valley (Fig. 4, 7D). This sample was 46 ft (14 m) above sea level and probably dates waning glaciomarine sedimentation in the study area.

The waning Puget ice lobe was partly buoyed by marine water, and thus a majority of Everson deposits are glaciomarine. Earlier studies of Everson deposits emphasized low-density, fossiliferous ‘dropstone’ diamicton as the dominant marine strata (Armstrong and Brown, 1954; Easterbrook 1962, 1963a,b, 1992). In this model, a rapidly thinning ice sheet/iceberg deposits mostly glaciomarine diamicton generally lacking lateral sedimentary facies changes. Our interpretations are consistent with deglaciation models and sedimentary facies analyses of Domack (1982, 1983, 1984), Pessl and others (1989), and Dethier and others (1995, 1996) that emphasize the diverse nature of these deposits and apply sedimentary facies models to account for the lateral and vertical variation in clay, silt, sand, and gravel and diamicton and fossil content. A complex interplay of glaciomarine and terrestrial depositional processes occurred in ice-marginal, fluvial-alluvial fan, marine fan, beach, lagoon, deltaic, and turbidite fan settings. Facies groups of the Everson Interstade are distinguished on the basis of sedimentary structures, textures, altitude relative to the glaciomarine limit, and internal stratigraphy. Everson sedimentary facies observed in the study area are (1) a mostly fine, ice-proximal to ice-distal glaciomarine facies (units $Qgdm_e$, $Qgdm_{ec}$, $Qgdm_{ed}$), (2) a mostly coarse, ice-proximal terrestrial to marine outwash and flow-till facies (units $Qgo_e$, $Qgom_e$, $Qgod_e$, $Qgt_e$), and (3) an emergence (beach) facies (unit $Qgom_{ee}$).

$Qgdm_e$, $Qgdm_{ed}$, $Qgdm_{ec}$ **Glaciomarine drift (Pleistocene)**—Undivided glaciomarine drift (unit $Qgdm_e$) locally divided into a clast-rich diamicton containing abundant dropstones (unit $Qgdm_{ed}$) and a silt- and clay-rich unit ($Qgdm_{ec}$) with few or no dropstones. Glaciomarine drift is light yellow-brown and blocky and stiff when dry and dark brown to grayish blue and soft when moist or wet. It locally has vertical jointing or desiccation cracks, as well as lenses or layers of loose outwash sand and gravel. Unit $Qgdm_{ed}$ is diamicton consisting of silty sandy gravelly clay to clayey gravel. It is typically massive or crudely stratified on a scale of several meters and has a varying gravel dropstone content. Unit $Qgdm_{ec}$ consists of moderately to well-sorted sandy silt, sandy clay, clayey silt, or clay that lacks or contains only rare gravel, cobble, or boulder dropstones. Unit $Qgdm_{ec}$ is massive or, less commonly, occurs as varved or laminated rhythmites. (See Dragovich and others, 1998; Dragovich and Grisamer, 1998; or Easterbrook, 1962, for criteria to differentiate till and glaciomarine drift.)

$Qgo_e$ **Terrestrial to marine recessional outwash (Pleistocene)**—Terrestrial outwash (unit $Qgo_e$) consisting of loose, angular to subrounded sand, sandy gravel, gravelly sand, and sandy cobbly gravel locally with boulders; rare interlayered thin to very thin beds of sandy silt and silt. Sands are typically light olive-gray when dry and dusky yellow when weathered; commonly displays subhorizontal beds crudely defined by variations in cobble, gravel, and sand content, typically 2 to 3 feet (~1 m) thick; local low-amplitude foreset or trough cross-bedding. Beds commonly display pebble imbrication and scour bedding indicative of a fluvial braided-channel environment and locally dip slightly west toward the ancient Skagit River embayment.

$Qgod_e$ **Deltaic outwash complex (Pleistocene)**—Moderately to well-sorted, loose sand and sandy gravel with concentrations of cobbles; beds are typically inches to several feet thick. Bottomset beds are mostly glaciomarine drift rhythmites. High-amplitude planar foreset beds, indicative of deltaic deposition, are exposed in the NW¼ sec. 16, T33N R4E, and SW¼ sec. 22, T33N R4E. The deltaic complex forms an outwash valley train along State Highway 534 between Conway and Lake McMurray with the open Puget Lowland to the west (Plate 1).

$Qgom_e$ **Glaciomarine outwash (Pleistocene)**—Loose, subrounded to angular sandy gravel, gravelly sand, sand, silty sand, and lesser sandy cobble gravel with interlayered silt beds. Average grain size is smaller in this unit than in terrestrial or deltaic outwash. Locally thinly laminated to varved; contains silt-sand couplets similar to the rhythmically bedded glaciomarine outwash described by Domack (1984) and Dragovich and others (1999, 2000b). Intimate interlayering with glaciomarine drift indicates submarine deposition for most areas mapped as unit $Qgom_e$, although it may locally include terrestrial outwash deposits. Terrestrial ablation or flow ‘till’ is locally associated with outwash and typically consists of soft to stiff clayey or silty diamicton; may include moderately to poorly sorted, silty sandy gravel or sandy boulder-cobble gravel deposits with some silt. These sediments were probably deposited by ice marginal depositional mechanisms, including ablation and mass-flow. Unit is locally associated with both kettle topography and oversteepened bedding (40–80°) indicative of ice shove or collapse within dead-ice terrain.

$Qgom_{ee}$ **Emergence (beach) deposits (Pleistocene)**—Loose sand and gravel that ranges from massive to distinctly stratified; locally associated with topographic benches or subtle wave-cut terraces. Many Everson glaciomarine outcrops are topped with up to 3 ft (1 m) of emergence sands or gravels that reflect temporary beach reworking of the substrate during isostatic emergence. Longer sea-level stands produced more distinctive

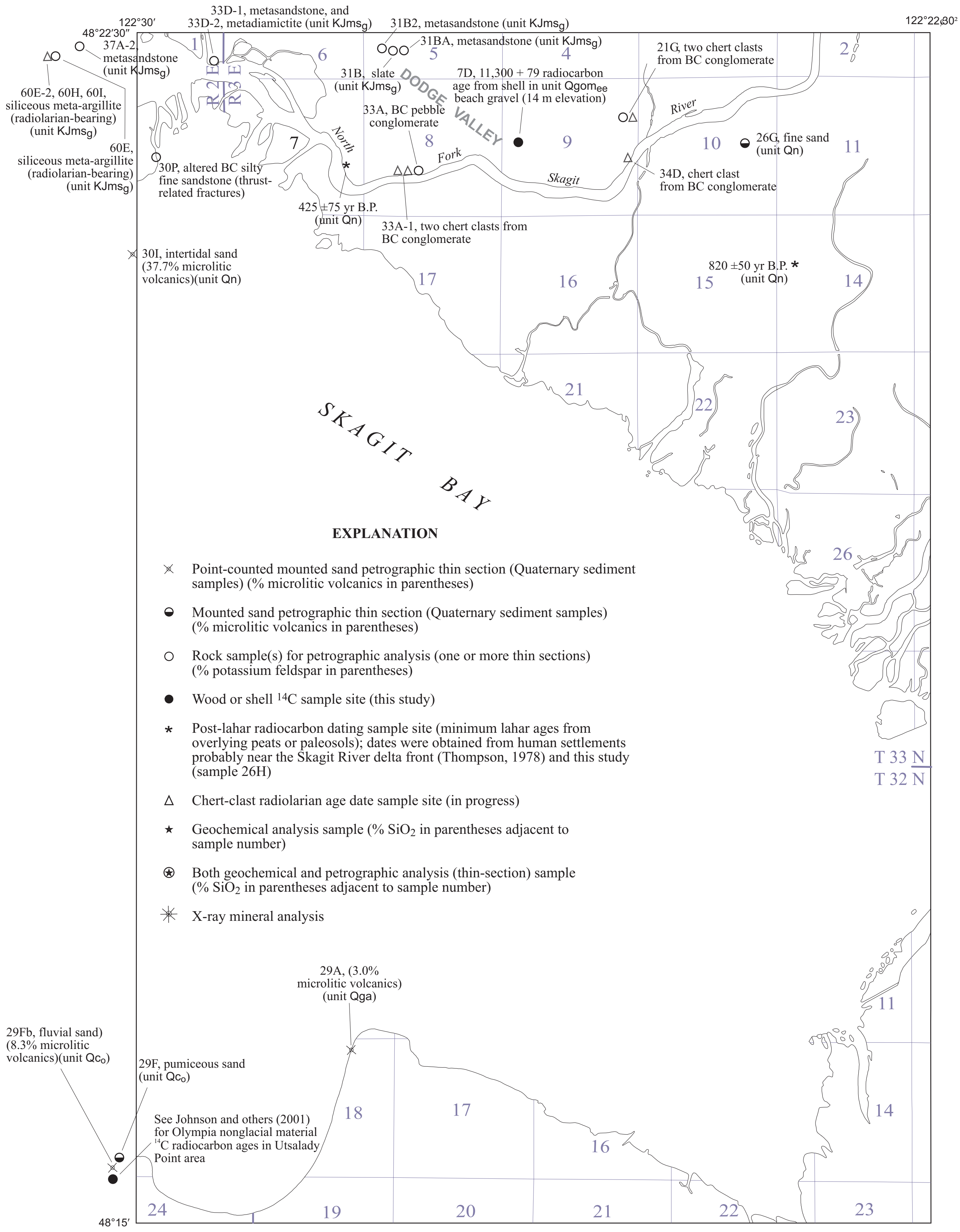


**Figure 4.** Sample site locations in and near the Utsalady quadrangle *(this page)* and Conway quadrangle *(facing page)*. (See Appendices 1–3.) We also show the location of radiocarbon samples from previous studies (Johnson and others, 2001; Thompson, 1978; Dethier and others, 1995).

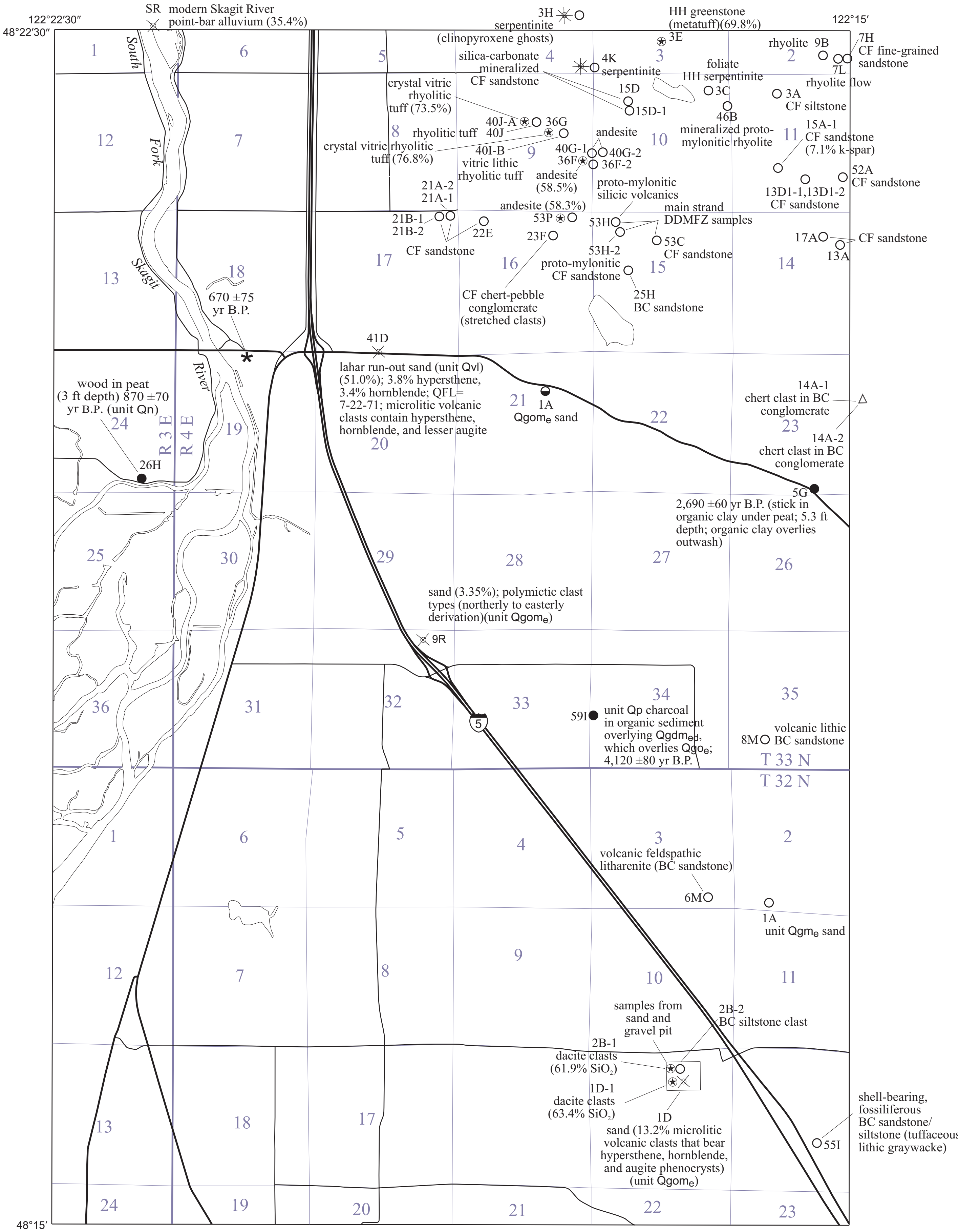


Percent with some symbols is the point-count percentage of dacitic lithic clasts (Appendix 2). We also show the percent $SiO_2$ for the geochemical samples (Appendix 3). BC, rocks of Bulson Creek; CF, Chuckanut Formation; HH, Helena–Haystack mélange.

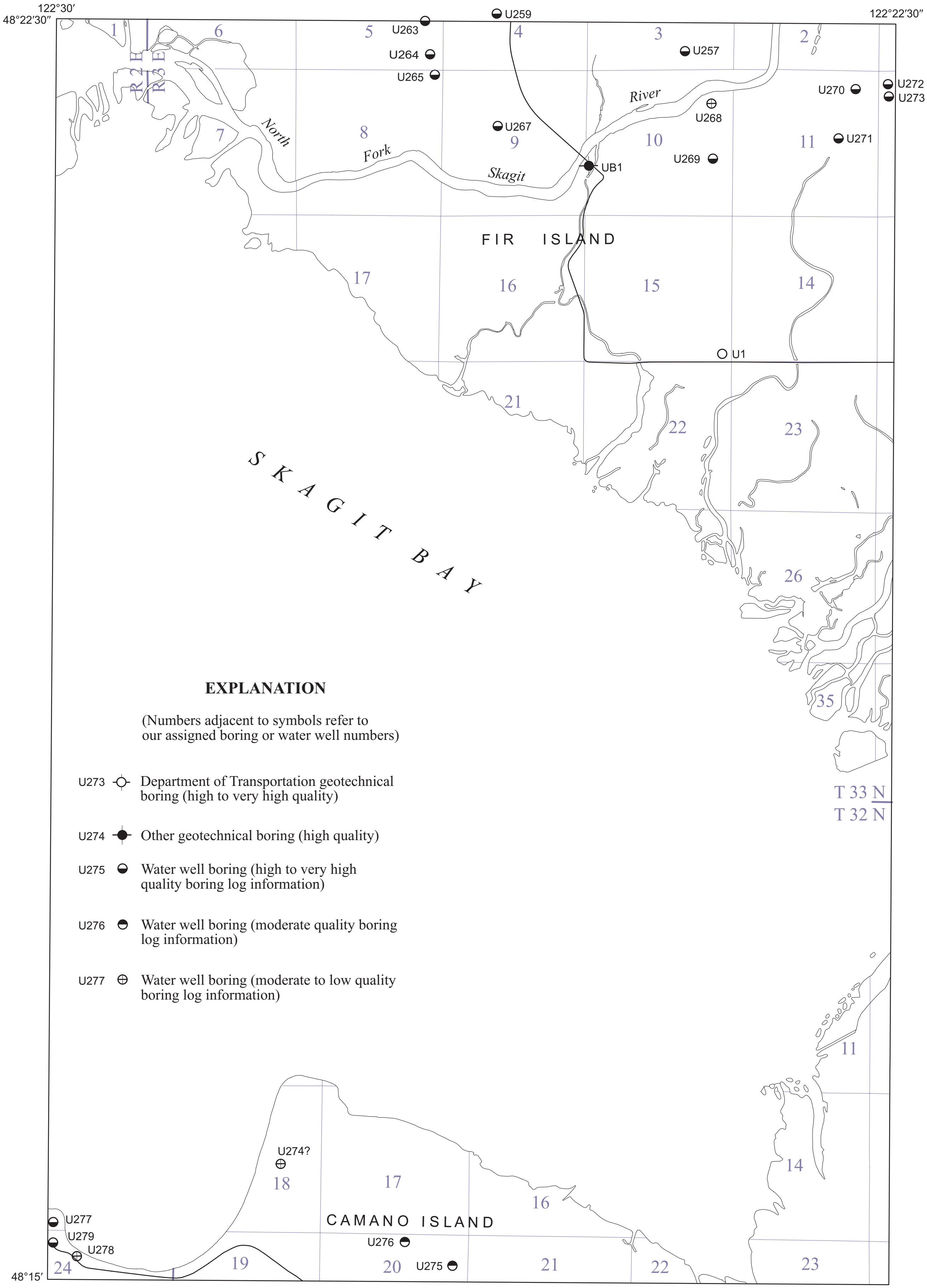


**Figure 5.** Location of water wells and geotechnical borings in the Utsalady *(this page)* and Conway *(next page)* quadrangles. The cross sections on Plate 2 were constructed using some of the water-well data, but much of the water-well data is low quality and thus was not used.

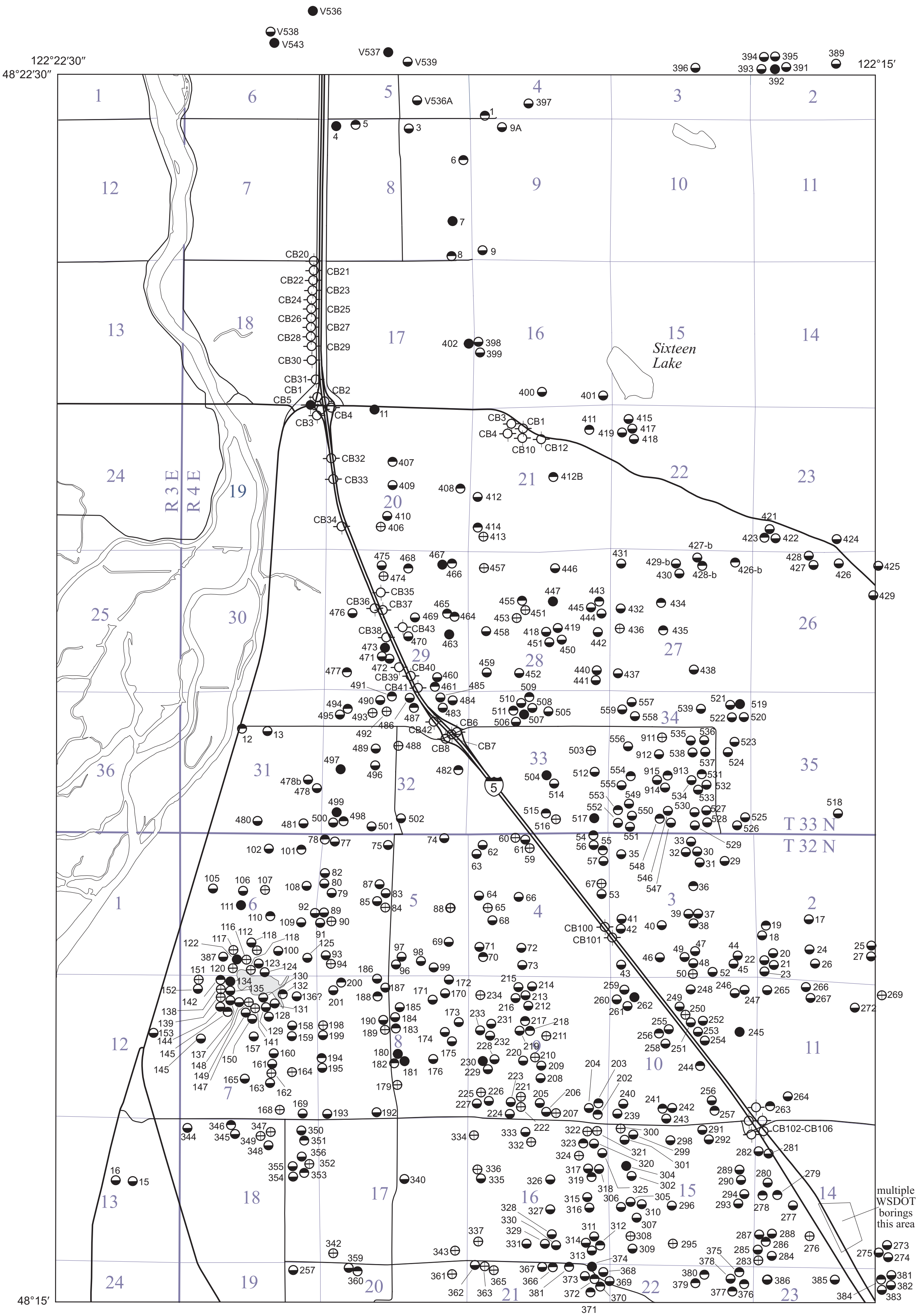

122°22′30″
48°22′30″
122°15′
48°15′
Sixteen Lake
R 3 E
R 4 E
T 33 N
T 32 N
5
multiple WSDOT borings this area

'strandlines' (Fig. 2). (See Siegfried, 1978, for a discussion of the stratigraphy of raised marine terraces north of the study area.)

### *Vashon Stade*

$Qgt_v$ **Till (Pleistocene)**—Nonstratified, dense to very dense diamicton consisting of clay, silt, sand, and gravel in various proportions, with scattered cobbles and boulders; rare lenses of sand or gravel; dark yellowish brown to brownish gray. Some clasts derived from the Coast Plutonic Complex of British Columbia (Easterbrook, 1962). Till unconformably overlies bedrock, advance outwash, and much less commonly, older glacial and nonglacial units (Plate 2, cross sections D–J). Below the glaciomarine limit of 340 to 400 ft (104–122 m) elevation, Vashon till very commonly underlies glaciomarine drift. Radiocarbon dates from outside the study area indicate an age between 17,000 and 13,600 yr B.P. Subsurface data indicates that Vashon till is locally in excess of 100 ft (30 m) thick in the Conway quadrangle (Plate 2, cross sections D–J). We interpret these thick deposits as the result of an extensive and buried dead-ice terrain in which lodgment till, ablation, and (or) flow till were all deposited, resulting in a thick composite section of diamicton. (See Dragovich and others, 1998; Dragovich and Grisamer, 1998; or Easterbrook, 1962, for criteria to differentiate till and glaciomarine drift.)

$Qga_v$ **Advance outwash (Pleistocene)**—Stratified, moderately to well-sorted, moderately to very dense, medium to coarse sand, pebbly sand, and sandy gravel, with minor amounts of fine silty sand or sandy silt, and clay interbeds with scattered lenses and layers of pebble-cobble gravel; thinly to very thickly bedded with subhorizontal bedding or generally south-dipping cross-stratification (Plate 1); localized cut-and-fill structures and trough and ripple cross-beds; thinly bedded silts locally display overturned folds with an overall fold geometry consistent with north to south (simple) shear folding during Vashon ice advance. Sands are typically medium or light gray when dried and weather tan or pale yellowish brown. Point count data (sample 29A, Appendix 2, Table B) indicate sand grains are mostly quartzo-feldspathic lithic clasts (~21%), quartz-mica tectonite, greenstone, and greenschist undivided metamorphic lithic clasts (~19%), monocrystalline quartz, polycrystalline quartz, and chert (~27%), plagioclase (~13%), and sedimentary lithic clasts (~8%). This sample appears to have a Coast Mountains (B.C.) quartzo-feldspathic granitic and metamorphic provenance, with lesser locally derived clasts.

$Qgl_v$ **Transitional beds (Pleistocene)**—Silt and clay deposits underlying Vashon advance outwash. This rarely exposed unit consists of glacial and (or) nonglacial deposits; typically moderately dense to dense, well-sorted, very thin to thick beds of clay, clayey silt, silt, and sand (Plate 2, cross sections D, E, G, H, J). The unit is composed of massive to laminated silt with lenses of sand in sec. 18, T32N R4E. Pessl and others (1989) correlated their 'transitional beds' with undifferentiated early Vashon advance outwash and (or) late nonglacial sediments deposited in local low-energy basins. Unit $Qgl_v$ lacks organic layers. We separated the transitional beds from the underlying nonglacial beds that typically contain layers and lenses of organic materials such as peat. On the basis of stratigraphic position and areal extent, some of the fairly thick deposits (>100 ft or 30 m) appear to be early Vashon Stade glaciolacustrine deposits. These deposits may be lithologically correlative with the basal part of early Vashon advance outwash deposits, such as the Lawton Clay Member of the Vashon Drift near Seattle (Mullineaux and others, 1965). Unit $Qgl_v$ is stratigraphically similar to both the fine deposits under advance outwash in the Anacortes area (Dragovich and others, 2000c, unpub. data) and the Pilchuck Clay Member of the Vashon Drift of Newcomb (1947). Newcomb indicated that the Pilchuck clay "consists largely of finer materials that seem to have accumulated in slack waters, probably impounded against the mountains along the inner margin of the advancing Vashon ice." Advance outwash on the glaciated uplands of the Conway quadrangle is commonly less than 30 ft (9 m) thick or locally absent. This may be indicative of a lateral facies change from coarse fluvial advance outwash to fine lacustrine beds represented by unit $Qgl_v$. (See Fig. 6 and Plate 2, cross sections D–J, and compare with stratigraphic thickness data of Dragovich and Grisamer, 1998.)

## Deposits of the Olympia Nonglacial Interval

Nonglacial deposits are well exposed only along the lower portions of some coastal bluffs but are widespread in the subsurface of the glacial uplands (Plate 2, cross sections D–J). (See Dragovich and Grisamer, 1998.) Fine-grained distal advance outwash or lacustrine deposits of the Vashon Stade conformably overlie the silt and clay strata of the Olympia nonglacial interval. As a result, obscure contacts between Olympia nonglacial and early Vashon units are the norm. (See unit $Qgl_v$.) Organic materials are rare in glacial deposits, but common in nonglacial sequences due to the relatively high organic productivity during nonglacial intervals. The Olympia nonglacial interval is separated from the overlying deposits on the basis of its higher organic sediment content. The Olympia nonglacial interval occurred between about 21,000 and 60,000 yr B.P. (Mullineaux and others, 1965; Deeter, 1979)(Plate 2). Johnson and others (2001) obtained a $^{14}C$ age of 21,110 yr B.P. for Olympia deposits at Utsalady Point directly southwest of the study area (Fig. 4); Dragovich and others (2000c) and Pessl and others (1989) have also obtained $^{14}C$ ages for the Olympia nonglacial interval near the study area.

$Qc_o$ **Olympia nonglacial deposits (Pleistocene)**—Compositionally heterogeneous unit composed of dense to very dense, gray to buff sand, gravelly sand, organic-rich sand, silty sand, silt, silty clay, and peat, with minor gravel and cobble gravel and rare diamicton of probable mass-flow origin; disseminated organic material, logs, or wood fragments are common. Unit is typically well sorted, locally iron-stained, and rarely slightly cemented; characteristically very well stratified and very thinly to thickly bedded; some well-laminated horizons have a fissile aspect. Sedimentary structures include plane laminations, scour and fill, trough cross-bedding, flame structures, and ripples.

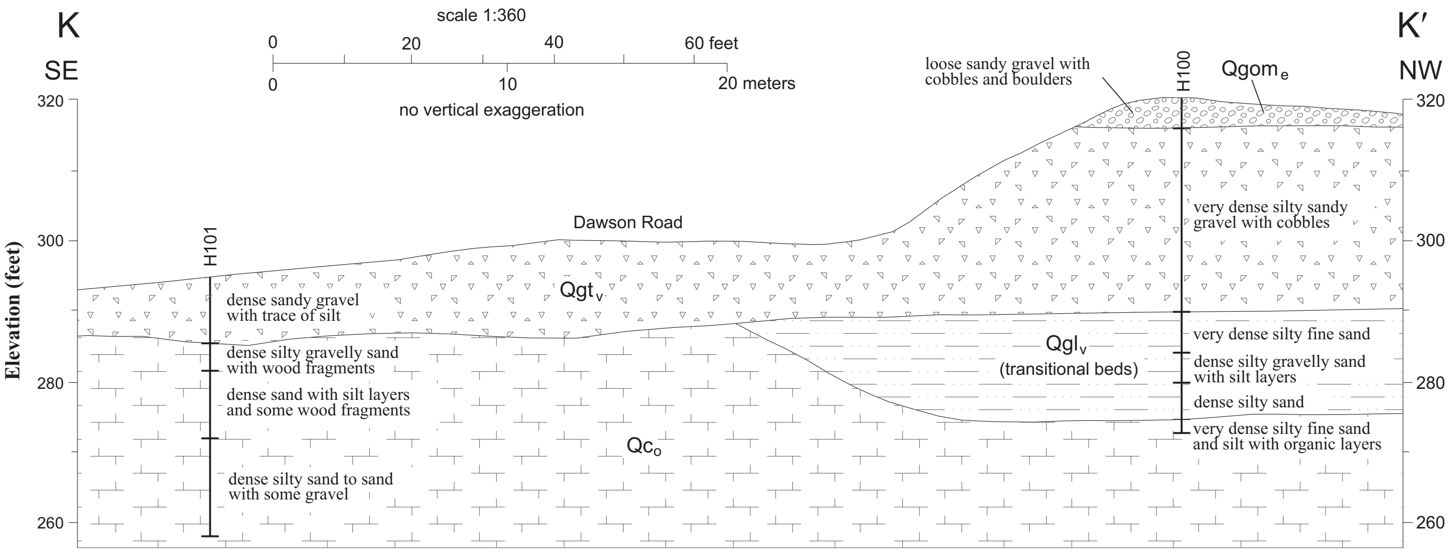


**Figure 6.** Cross section K–K′ constructed using Washington State Department of Transportation I-5 overpass geotechnical boring log information. Note the lack of coarse-grained advance outwash (unit Qga$_v$) underneath the Vashon glacial till (unit Qgt$_v$). Unit Qgl$_v$ (transitional beds) may be either distal advance outwash or Olympia nonglacial beds (unit Qc$_o$) that lack the characteristic layers or lenses of wood, peat, or undifferentiated organics characteristic of the nonglacial beds.

Most Olympia nonglacial sediments were deposited in a meandering river environment. At Utsalady Point (Fig. 4, site 29F; Johnson and others, 2001), sandy gravel channel deposits occur in a thick stratigraphic section of fluvial sands, silts, and peats. The fluvial sands are compositionally heterogeneous but most are of mixed local metamorphic to eastern volcanic provenance. Most distinctive is the occurrence of hypersthene-bearing dacitic fragments in the sands and lenticular beds of pumice lapilli of apparent homogeneous composition (Fig. 4, sample 29F). A point-counted sand sample from Utsalady Point (Fig. 4, Appendix 2, site 29Fb) contains 8 percent microlitic hypersthene-hornblende dacite fragments. These volcanic clasts are similar to Glacier Peak dacitic lithic fragments observed in the Skagit River alluvial sand and provide evidence that Glacier Peak has been contributing sediment to the Puget Lowlands for at least 20,000 years.

### Possession Glaciation (cross sections only)

ot **Older till (Pleistocene)**—Clay, silt, sand, and gravel in various proportions, with scattered cobbles and boulders; may locally include glaciomarine drift. We do not assign a formal geologic symbol to this unit in order to emphasize the tentative nature of this correlation with Possession Glaciation.

oo **Older outwash (Pleistocene)**—Pre-Fraser glacial or nonglacial sediments mostly composed of sand and gravel with lesser clay or silt interbeds; alternatively, may locally be correlative with fluvial nonglacial deposits of the Whidbey Formation of Easterbrook (1994). We do not assign a formal geologic symbol to this unit in order to emphasize the tentative nature of this correlation with Possession Glaciation.

### Whidbey Nonglacial Interval (cross sections only)

Qc$_w$ **Whidbey nonglacial deposits (Pleistocene)**—Mostly sand with interbeds of silt, clay, sandy clay, and silty clay with local gravel lenses; peat and wood are common. Hansen and Mackin (1949) interpreted the depositional environment as slowly aggrading meandering streams and adjacent flood plains.

### Double Bluff Glaciation (cross sections only)

oot **Till (Pleistocene)**—Compact till and diamicton interbedded with sand and silt (Easterbrook, 1994). We do not assign a formal geologic symbol to this unit in order to emphasize the tentative nature of this correlation with Double Bluff Glaciation.

ooo **Outwash (Pleistocene)**—Gravel and moderately well-sorted, cross-bedded sand. We do not assign a formal geologic symbol to this unit in order to emphasize the tentative nature of this correlation with Double Bluff Glaciation.

## Tertiary Sedimentary and Volcanic Rocks

The broad Darrington–Devils Mountain fault zone (DDMFZ) traverses the northern portion of the Utsalady and Conway quadrangles (Plates 1 and 2). Mountain- and outcrop-scale structures and microstructures provide evidence that the Tertiary DDMFZ in the study area is a flower structure in a transpressional left-lateral strike-slip fault zone (Plate 2, cross sections A–C; Dragovich and Gilbertson, unpub. data).

## ROCKS OF BULSON CREEK

The rocks of Bulson Creek (Bulson Creek, herein) were first described by Danner (1957) and informally named by Lovseth (1975). Marcus (1981) divided the unit into a lower 1,200-m-thick conglomerate lithofacies and an upper finer grained lithofacies at least 550 m thick. Our units $\Phi Ec_{bcg}$ and $\Phi Ec_{bs}$ correspond to these lower and upper lithofacies, respectively. Marcus concluded that the lower lithofacies was deposited in alluvial fan to fluvial environments. The rocks of Bulson Creek occur directly south of the main strand of the DDMFZ. It seems likely that Tertiary vertical or oblique offset along the DDMFZ produced the relief necessary to create the Bulson Creek alluvial fan depositional environment. The upper, finer lithofacies was deposited in nearshore or shallow marine water as indicated by overall stratigraphy, sedimentary structures, and shallow water marine megafossils. The presence of these marine fossils and terrestrial plant fossils in the upper portion of the upper lithofacies requires a transition from a fluvial to an estuarine or nearshore marine environment.

The contact between the upper and lower lithofacies is not exposed in the study area. Marcus (1981) stated that the lower lithofacies was folded along an east–west axis prior to the deposition of the upper lithofacies and therefore the two lithofacies are separated by an angular unconformity. Conversely, Whetten and others (1988) suggested locally faulted and (or) interfingering lithofacies contacts. Both units are structurally juxtaposed against older units or depositionally overlie them. Outside the study area, the Bulson Creek rocks unconformably overlie paleosols developed on pre-Tertiary rocks and in some places are in fault contact with pre-Tertiary rocks (Marcus, 1981). Within the study area, we infer that the rocks of Bulson Creek are in both high- and low-angle (thrust) fault contact with the Tertiary rocks of the Chuckanut Formation (Plate 2, cross sections A–C).

Marine macrofossils in the upper lithofacies indicate an Eocene to late Oligocene age (Lovseth, 1975; Marcus, 1981). South of the study area, foraminiferal assemblages indicate an Oligocene Zemorrian Stage through upper Eocene to lower Oligocene Refugian Stage (Rau and Johnson, 1999). No other direct age constraints exist for the Bulson Creek rocks. However, several indirect constraints concur with this age range (Plate 2). For example, the lesser degree of folding and tilting (Plate 1) of the Bulson Creek beds suggests a younger age than the tightly folded Eocene Chuckanut Formation. Moreover, the Chuckanut Formation is locally intruded by Eocene volcanic rocks (unit Evr) and thus must be at least partially older than these bodies. Zircon fission track dates for unit Evr range from 41.5 ±3.4 to 52.7 ±2.5 Ma (Lovseth, 1975; Dethier and Whetten, 1981; Whetten and others, 1988). Available age constraints may allow for some overlap of units Evr and Bulson Creek (Plate 2). In order for units Evr and the lower lithofacies to overlap in age, unit Evr must be, at least locally, about 38 Ma or younger (S. Y. Johnson, USGS, written commun., 2002). Marcus (1981) reported rhyolite clasts in conglomerate beds; these clasts may have originated from unit Evr silicic volcanic rocks and may provide a maximum age for the unit. We agree that the intermediate to silicic volcanic lithic-rich nature of many of the sandstone and conglomerate clasts in both lithofacies suggests a volcanic provenance similar to unit Evr. This observation places constraints on both the age of Bulson Creek and the amount of strike-slip faulting across the DDMFZ. However, it does not necessarily indicate that the Bulson Creek rocks are younger than the silicic volcanic source rocks. Indeed, the distinctly volcanic lithic nature of some of the clast sources indicates direct volcanism or volcaniclastic sedimentation into the Bulson Creek basin. Certainly the volcanic-rich nature of some of the sandstones in the Bulson Creek argues for syndepositional volcanism.

$\Phi Ec_{bs}$ **Upper lithofacies (Oligocene to Eocene)**—Moderately well sorted, subangular to subrounded, coarse- to medium-grained sandstone with lesser interbeds of conglomerate, pebbly sandstone, siltstone, fossiliferous siltstone, coal, and shale. Sandstone is stained various shades of yellow and brown; siltstone and shale are reddish brown to pale olive. Most conglomerates and pebbly sandstones are massive, commonly imbricated, and contain subangular to subrounded clasts to 8 in. (20 cm) long. Sandstones are massive, but locally display well-developed cross-beds and crudely defined horizontal beds. Channel fills (10–65 ft or 3–20 m across) have weakly graded beds and localized scour-and-fill and cross-bedding structures. Siltstone and shale are laminated, and structures include simple, wavy, and flaser beds and current ripple marks.

We petrographically examined several siltstones and sandstones from the upper Bulson Creek lithofacies (Fig. 4). These rocks are commonly distinctly volcanic lithic and locally contain texturally immature ‘graywackes’. Tuffaceous and fossiliferous siltstone and very fine grained sandstone (site 55I, Fig. 4) consist of subangular to angular clasts (0.01–0.1 mm, 60%) in a dark brown semi-opaque matrix with iron oxide (39%). Dominant clast types are quartz, plagioclase, and volcanic lithic clasts; detrital augite is a minor component. Sandstones (samples 6M and 8M, Fig. 4) are classified as moderately to very well sorted volcanic-feldspathic litharenite or wacke to volcanic litharenite (volcanic sandstones). These samples consist of subangular to rounded clasts (0.1–2 mm, 85–95%) in a semi-opaque brown matrix locally containing iron oxide (4–16%). Dominant clast types are intermediate to siliceous microlitic volcanic clasts (10–98%). Some of the volcanic clasts contain quartz phenocrysts; other volcanic components are detrital volcanic quartz and minor augite. Marcus (1981) point-counted several upper lithofacies sandstones and reported lithic volcanic fragments in the range of 20 to 66 percent. Our petrographic observations confirm that some of the sandstones are volcanic sandstones and locally contain volcanic lithic clasts in excess of 90 percent. The source of this volcanic detritus may be unit Evr found regionally along the DDMFZ.

**Figure 7.** *(facing page)* Bedrock top elevation map for the Conway quadrangle. (Note: Contours above or below or at present day sea level may be distinguished by differing line types.) Many of the wells shown on Figure 5 either penetrated bedrock or are sufficiently deep to provide useful minimum bedrock depths. Subsurface bedrock morphology was further determined by projecting subsurface information obtained from a seismic reflection study performed directly north of the study area (Interpre’Tech/SeisPulse, LLC, 1996). Compare bedrock elevations with topography provided on the geologic map of the quadrangle (Plate 1) to obtain an estimated depth of Quaternary sediments in any given area. Note the northwest structural grain suggested by the bedrock elevation contours. This grain reflects the dominant northwest strike of bedding in the sedimentary rocks of Bulson Creek.

**EXPLANATION**

exposed bedrock

fault (dotted where concealed)

thrust fault

-100 / 0 / 100 inferred elevation of top of bedrock (feet above or below present sea-level); line types differ for contours above, below, or at sea level

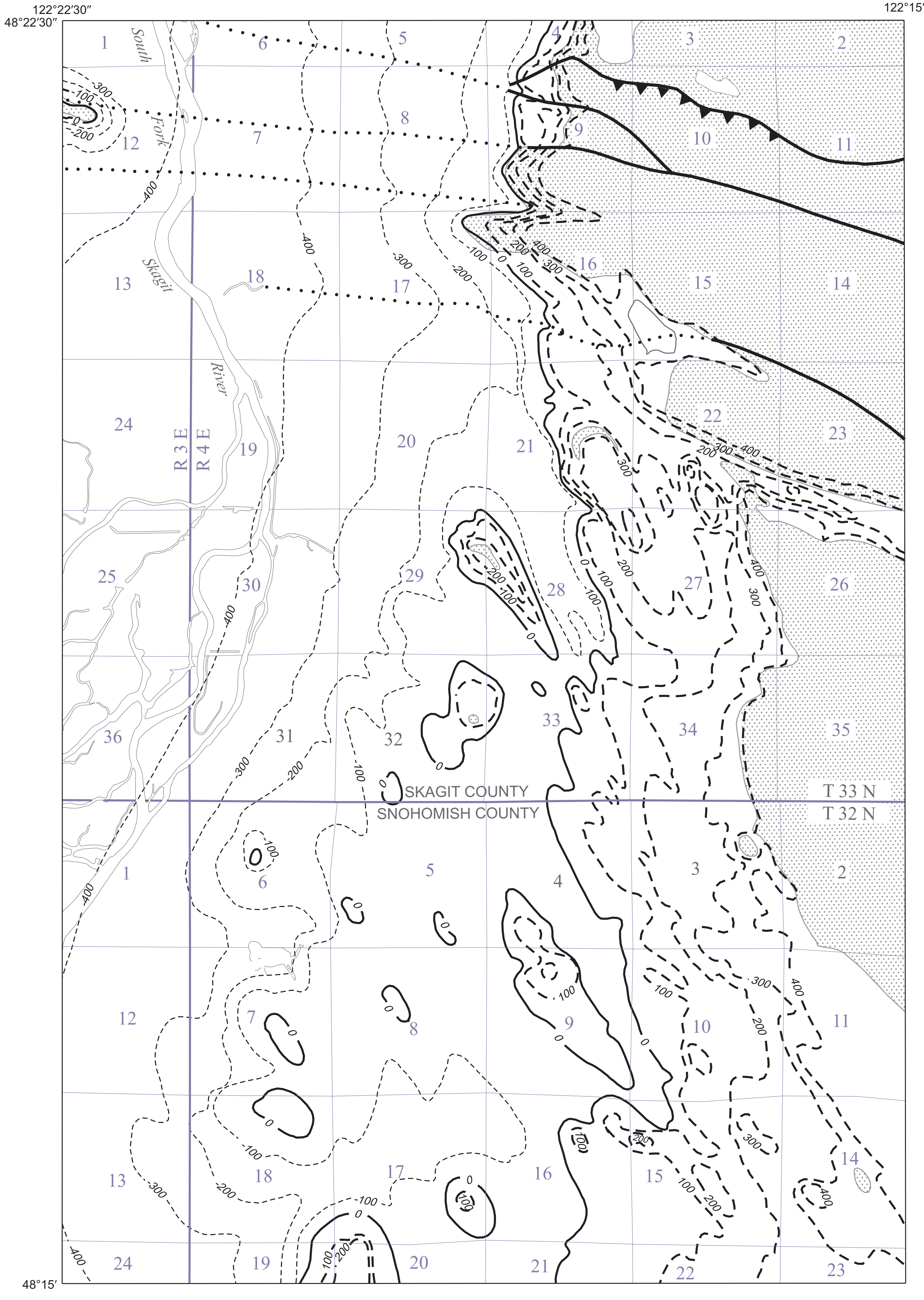
122°22′30″
48°22′30″
122°15′
48°15′
South Fork Skagit River
R 3 E
R 4 E
SKAGIT COUNTY
SNOHOMISH COUNTY
T 33 N
T 32 N

$\Phi Ec_{bcg}$ **Lower conglomeratic lithofacies (Oligocene to Eocene)**—Mostly yellowish brown, subangular to subrounded, moderately spherical to elongate, pebble and cobble conglomerate; typically massive to locally very thickly bedded; contains lesser interbeds of brownish gray or yellowish brown pebbly sandstone to sandstone, reddish gray siltstone, and minor diamictite and coal; reddish brown to yellowish brown color due to iron oxide staining. Conglomerates are typically structureless but locally display clast imbrication and subtle to distinct normal grading. Sandstone interbeds contain angular to subrounded clasts and vary from structureless to thickly bedded with rare graded bedding, channeling, and festoon cross-bedding. Carbonized leaves and branches occur in the sand and silt interbeds.

Conglomerate is greenish gray to yellowish brown and locally has reddish or yellowish brown oxidation. Clasts are as large as 1.6 ft (0.5 m) in diameter, but more commonly range from 0.8 to 2.8 in. (2–7 cm). Clast size generally decreases away from the main strand of the DDMFZ. Clasts commonly have a deep weathering rind; a few occur as highly weathered 'ghost' clasts. Most samples are poorly indurated and crumbly due to relatively poor cementation; rarely well indurated due to calcite cementation. Conglomerate clasts in alluvial fan channel and point bar deposits are commonly supported by a matrix of coarse sand; locally clasts are supported by brown to yellowish brown clay with disseminated fine to medium sand. These are classified as diamictites of probable mass-wasting origin and are probably debris flows in an alluvial fan depositional environment. Conglomerates are locally penetratively deformed in the DDMFZ. A well-sorted chert-pebble conglomerate (site 33A, Fig. 4) contains stretched pebbles with extensional veins of quartz and calcite and consists of subangular to subrounded, gravel-size clasts up to 1.2 in. (3 cm, 95%) of dark gray chert containing radiolarian ghosts, minor granitic clasts, and monocrystalline and polycrystalline quartz and chert sand-size grains (0.1–1 mm) set in a matrix of pink cement consisting of quartz (3%), iron oxide (2%), and calcite (15%).

Sandstones are classified as moderately to well-sorted feldspathic litharenite and consist of subangular to subrounded clasts (1–2 mm, ~95%) composed of chert, volcanic lithic fragments, and monocrystalline quartz (5–13%), polycrystalline quartz (12–33%), plagioclase (4–12%), potassium feldspar (0–15%), volcanic lithic clasts (8–15%), sedimentary lithic clasts (20–42%), and secondary white mica, quartz, and iron oxide. Sandstones also contain minor pyroxene, amphibole, garnet, and rutile, as well as sparse lithic clasts including serpentinite and detrital olivine derived from local bedrock sources (Marcus, 1981; this study, Fig. 4, sample 25H). A very fine sandy siltstone (sample 30P, Fig. 4) consists of subangular to subrounded clasts (0.01–15 mm, ~95%) mostly composed of quartz and plagioclase with minor potassium feldspar set in a matrix of semi-opaque iron oxide and a dark brown amorphous material (~30%). Typical of many of the sedimentary rock formations in the study area, the siltstone contains secondary white mica and calcite (~12%).

Our petrographic examination of the lower Bulson Creek lithofacies indicates that these rocks are generally compositionally more mature than the upper lithofacies (for example, they contain more chert, quartz, and feldspar and fewer lithic clasts). The varied composition over short distances indicates a dynamically changing source area and (or) varied sedimentation conditions over time. Clasts are mostly locally derived granite, rhyolite[1], phyllite, andesite, chert, sandstone (Chuckanut Formation), and greenstone. However, Whetten and others (1988) and Marcus (1981) noted that some beds contain abundant K-feldspar, suggesting a more distant source.

## VOLCANIC ROCKS

Various Eocene volcanic rocks crop out in the Chuckanut Formation (CF) along the Darrington–Devils Mountain fault zone (DDMFZ) in the northern third of the Conway quadrangle. Eocene volcanic rocks in and near the study area consist mostly of andesitic, dacitic, to rhyolitic flows, tuffs, and various hypabyssal intrusives bodies including domes and dikes (Lovseth, 1975; Whetten and others, 1988).

Ages for the volcanic rocks in the study area have been inferred from correlative volcanic rocks in adjacent quadrangles. C. W. Naeser (written commun., 1979, in Whetten and others, 1988) obtained a fission-track age on zircon of 52.7 ±2.5 Ma (early Eocene) from rhyolite tuff interbedded with sandstone from a quarry south of Table Mountain (SE¼ sec. 14, T33N R5E), and Lovseth (1975) dated zircon in rhyolite from the Hendricks quarry near Big Lake at 41.5 ±3.4 Ma by the same method. J. Vance (pers. commun. to Lovseth, 1975) also obtained a fission-track age of 43.5 Ma from rhyolite east of the study area. A tuff in the Chuckanut Formation near Mount Vernon north of the study area has a revised fission-track age of 52.6 ±4.8 Ma (R. W. Tabor, pers. commun. to Evans and Ristow, 1994). However, andesite dikes locally intrude the rhyolite (Lovseth, 1975; this study) and thus are mostly younger than the rhyolite. Microlitic siliceous volcanic fragments with eutaxitic texture and pyroxene crystals occur in the Bulson volcanic sandstones and may be evidence of synvolcanic andesitic detritus entering the Bulson basin.

Although contacts of volcanic rocks with other units in the study area are not well exposed, field relations indicate that the volcanic rocks are both intrusive into and faulted against the Chuckanut Formation (Plate 1; Lovseth, 1975). An intrusive relation is petrographically confirmed by the occurrence of Chuckanut siltstone and sandstone xenoliths in rhyolite (sample 40I-B, Fig. 4). East of the study area, ash-flow tuff, intrusive rhyolite, and minor andesite flows occur in the Chuckanut

[1] Marcus (1981, p. 71) indicated that rhyolite clasts in the rocks of Bulson Creek south of the DDMFZ are petrographically similar to unit Evr north of the DDMFZ. However, silicic volcanic rocks are common along much of the DDMFZ (for example, Evans and Ristow, 1994), indicating that unique piercing points along the DDMFZ are not yet available using the distribution of Tertiary volcanic rocks of the region. Although many kilometers of left-lateral displacement on the DDMFZ displaced source rocks north of the DDMFZ from the Bulson Creek basin, westerly paleocurrent measurements of Marcus (1981) show that the materials in the upper lithofacies of Bulson Creek fluvial rocks were transported along the DDMFZ. Thus, although a direct link cannot be made between units Evr and the rocks of Bulson Creek, certainly siliciclastic volcanic events similar to those reflected by unit Evr influenced Bulson Creek basin evolution.

(Dethier and Whetten, 1980). Although tuffs occur as thin discrete beds in the Chuckanut Formation near the study area (Dethier and Whetten, 1980; Evans and Ristow, 1994), the Chuckanut in the study area (1) lacks tuffaceous interbeds, (2) is poor in volcanic lithic clasts, (3) shows no evidence of volcanic flows in or over sedimentary beds, and (4) lacks lateral facies transitions between the fluvial Chuckanut Formation and the volcanic rocks. Field relations suggest that unit Evr volcanic rocks are, at least in part, in fault contact with the Chuckanut along the DDMFZ. It seems likely that initial intrusive emplacement of the volcanic rocks was partially controlled by preexisting strands of the DDMFZ; later continued faulting along the DDMFZ locally imbricated the volcanic bodies, leading to intrusive, faulted, and rare conformable(?) depositional contacts with the Chuckanut Formation.

Evr **Andesitic to rhyolitic volcanic rocks (Eocene)**—Volcanic rocks in the study area are andesites and rhyolites (Fig. 4 and Appendix 3). Andesites (58–59% $SiO_2$, Appendix 3, Table B) include dikes and minor flows; gray to dark gray, altered or weathered yellow brown to greenish gray. Petrographic examination (Fig. 4; Appendix 3, Table A) indicates that the andesites are composed of interstitial quartz (125%, avg. 9%), euhedral to subhedral microlitic needles or microphenocrysts of plagioclase with rare ~1 mm-long blocky plagioclase grains (0–20%, avg. 6%), augite grains (0–38%, avg. 10%; ≤0.5 mm), and opaque minerals (6–15%) in a cryptocrystalline matrix of dark brown, tan, or yellow glass (1–36%, avg. 24%). Alteration mineral products include calcite (0–3%), iron oxide (0–7%), propylite (0–1%), and minor opal, chlorite, biotite, and epidote. Many of the andesites are dark colored due to abundant disseminated opaque minerals, some of which are probably alteration mineral products. Compared to the rhyolites, the andesites are relatively texturally homogeneous. Calcite- or opal-filled vesicles are common and locally flattened parallel to trachytic plagioclase microlites as a result of magmatic flow. Although field relations suggest that the andesite forms mostly dikes or sills, a vesicular flow top at site 36F (Fig. 4) is blocky and weathered red; flows overlie less vesicular and unweathered andesite, suggesting some subareal flow deposition. Andesite at site 36F consists of euhedral, acicular plagioclase laths (5–7%; 0.1–0.5 mm) and trace amounts of euhedral clinopyroxene (≤0.3 mm) in a matrix of microlitic plagioclase, clinopyroxene, glass, and an unknown aphanitic opaque mineral that may be devitrified glass (93–97%); plagioclase laths in this sample are mostly well-aligned and subparallel to elongated vesicles (≤1.2 in or 3 cm in length) that are filled with amorphous silica and calcite.

Rhyolites (73–77% $SiO_2$, Appendix 3, Table B) include crystal vitric and lithic vitric lapilli tuffs, flow breccia, and flows; light to dark gray, locally altered to pinkish gray or very pale brown; locally, strongly flattened volcanic clasts and pinkish flow tops suggest hot emplacement and welding. Petrographic examination of several samples (Fig. 4, Appendix 3, Table A) indicates that the rhyolites are composed of euhedral to embayed or resorbed subhedral quartz phenocrysts (8–30%, avg. 16%; 0.2–3 mm), euhedral to subhedral blocky plagioclase phenocrysts (1–30%, avg. 9%; 0.2–2 mm long), volcanic lithic fragments (0–38%, avg. 10%, ≤3 cm long; $An_{30-36}$), and opaque minerals (1–2%) in a cryptocrystalline matrix of brown to yellowish clear glass (33–76%, avg. 60%); alteration minerals include calcite (0–15%), iron oxide (0–3%), probable propylite (0–4%), and minor silica and pyrite. Rhyolite is commonly altered and Fe-stained, partly bleached or limonite-stained, and locally propylitically altered. Lovseth (1975) indicated that the groundmass is locally altered to chlorite and replaced by zeolite and quartz. Mineral-filled vesicles are common and conduit neck vesiculation and forceful emplacement is suggested by strong local vesicle flattening. Compositional banding, autobrecciated rhyolite clasts, and eutaxitic texture suggest subaerial flow. Compared to the andesites, the rhyolites are texturally diverse and commonly have an inhomogeneous appearance in thin section. Volcanic lithic clast types in tuffs and tuff breccias are commonly texturally diverse and include vesicular to nonvesicular andesitic varieties and rare light-colored pumice.

## SEDIMENTARY ROCKS OF THE CHUCKANUT FORMATION

Johnson (1982, 1984a) divided the Chuckanut Formation into the Bellingham Bay, Slide, and several other members. Mustoe and Gannaway (1997) and Dragovich and others (1997) include Bellingham Bay and Slide members in their informally named lower Chuckanut Formation. The lower Chuckanut is named the Coal Mountain unit east of the study area (Evans and Ristow, 1994). The Chuckanut Formation in the study area correlates well with the lower Chuckanut Formation of Johnson (1982) and Evans and Ristow (1994), especially in terms of potassium feldspar content, compositional maturity, and overall stratigraphic style. Johnson (1982) and Evans and Ristow (1994) reported at least 3 percent in the lower Chuckanut Formation, but sparse potassium feldspar in overlying members. Johnson (1982, 1984a) obtained a zircon fission-track age of 49.9 ±1.2 Ma from a dacite lithic-tuff bed near the top of the Bellingham Bay Member north of the study area. Reiswig (1982) assigned early middle to late Eocene ages to pollen collected from laterally correlative strata. On the basis of approximate source-terrane uplift ages implied by several detrital zircon fission-track ages from the base of the Bellingham Bay, Johnson (1982, 1984a) and Johnson and others (1983) suggested that the base of the Bellingham Bay could not be older than about 55 Ma and is probably younger. An Eocene age for most of the Chuckanut lithostratigraphic equivalents in western Washington and the central Cascades is consistent with radiometric ages of interbedded volcanic rocks (Johnson, 1984a; Evans and Ristow, 1994; Mustoe and Gannaway, 1997).

A meandering river and adjacent flood-plain depositional environment is indicated for the Bellingham Bay Member (Johnson, 1982, 1984a,b). Paleocurrent, fission-track, and provenance data suggest that the generally potassium-feldspar-rich arkosic sandstones of the lower Chuckanut Formation were derived from uplifted and eroded crystalline basement rocks east of the crystalline core of the Cascade Range, possibly the Omineca Crystalline Complex basement in north-central Washington (Johnson, 1984a). Faulting, uplift, and erosion of locally derived basement and transport of detritus into mostly fault-controlled fluvial basins are clearly documented for the upper Chuckanut Formation members (for example, Johnson, 1982, 1984a; Evans and Ristow, 1994; Mustoe and Gannaway, 1997; Dragovich and others, 1997). Although all Bellingham Bay Member samples are arkosic and distinctly less lithic and more potassium feldspar-rich than upper Chuckanut Formation sandstones, some samples in and near the study area contain detritus indicating uplift and a mild degree of exposure and erosion of local basement rocks, such as phyllite, greenstone, greenschist, and serpentinite (Robertson, 1981; Dragovich and others, 1999, 2000b; this study). We visualize mature, far-easterly provenance arkosic sediments of large meandering river basins interdigitating with locally derived detritus resulting from localized basin marginal faulting.

In the study area, the Chuckanut Formation is in fault contact with pre-Tertiary bedrock and the rocks of Bulson Creek and in fault and intrusive or depositional contact with Eocene volcanic rocks. Within the Darrington–Devils Mountain fault zone, Chuckanut Formation strata are intensely folded and locally overturned, and the sandstone is silicified and has developed a cataclastic texture. Outcrop-scale folds, conspicuous map patterns, and structural data indicate that the Chuckanut Formation has been locally thrust and deformed into a positive flower structure (Dragovich and Gilbertson, unpub. data; Plate 2, cross sections A–C).

$Ec_b$ **Chuckanut Formation (Eocene)**—Thick- to very thinly bedded, well-sorted, micaceous, medium- to coarse-grained feldspathic sandstone and minor conglomerate (coarse-grained intervals) alternating with mudstone and fine-grained feldspathic sandstone, siltstone, and minor coal (fine-grained intervals). Coarse- and fine-grained intervals are upward-fining cycles. Sandstones are light brownish gray to light gray; weather to very pale yellow or to brown. Coarse-grained interval sedimentary structures include trough cross-bedding, ripple lamination, or plane lamination; conglomerates are massive to crudely stratified. Fine-grained sedimentary intervals include mostly massive or laminated mudstone; sedimentary structures include ripples, flute casts, mottled horizons; plant fossils are common (Johnson, 1982, 1984a,b).

Sandstones are mostly well-sorted arkosic arenite. Dominant clast types in and near the study area include rounded to subangular monocrystalline quartz (18–40%), polycrystalline quartz and chert (13–18%), volcanic lithic clasts (4–6%), sedimentary lithic clasts (1–19%), plagioclase (2–17%), potassium feldspar (2–13%), as well as metamorphic lithic clasts, biotite, and muscovite (2–7%)(Frizzell, 1979; Marcus, 1981; this study; Appendix 2, sample 15A-1). Unaltered sandstone consists of subangular to subrounded clasts (0.1–1.8 mm, 81–99%), locally with some fine-grained matrix (0–5%). Slightly altered samples additionally have white mica (≤4%), Fe-chlorite (≤1%), and calcite (≤12%). Altered samples are reddish brown and contain up to 10 percent iron oxide. Distinctly mineralized and protomylonitically deformed sandstones near the thrust fault north of the main strand of the DDMFZ are yellowish red (Plate 1, Fig. 4, samples 15D and 15D-1).

Pebbly sandstone and conglomerates (samples 21G and 23G, Fig. 4) consist of rounded lithic clasts (70–90%), quartz (2–20%), potassium feldspar (0–3%), and white mica and Fe-chlorite (0–3%) in a matrix containing calcite and Fe oxides (0–15%). Conglomerate clasts are up to 0.8–1.2 in (2–3 cm) in length and are mostly chert and polycrystalline quartz; clasts are locally stretched and contain extensional veins and quartz pressure shadows. Pebbly sandstones are lithic arkose or feldspathic lithic arenite and vary from those with little or no potassium feldspar in the sand fraction to those with appreciable potassium feldspar, quartz, white mica, muscovite, and lithic clasts. Noteworthy is the increased compositional maturity in coarse-grained samples from fluvial channel facies. For example, pebbly sandstones typically contain mostly chert and monocrystalline quartz, with lesser feldspar and only minor or rare lithic fragments. Reddish brown, very fine sandy siltstone and siltstone consist of subangular to angular clasts primarily composed of monocrystalline quartz with plagioclase (0.05–0.5 mm, 60–80%) in an opaque matrix of reddish brown material (8–20%) and calcite cement and (or) veins (0–10%). Accessories include primary and secondary white mica (4–8%), iron oxide (2–4%), opaque minerals, zircon, and some quartz cement.

Chuckanut Formation rocks are hydrothermally altered and sheared or fractured where the main strand of the DDMFZ is exposed along and near Johnson Creek (Plate 1). Sheared rocks are protomylonites, mylonites, and cataclasites exhibiting both brittle and brittle-ductile microstructures and L, L-S, and S-C shear fabrics. White mica neomineralization during mylonitization defines a shear foliation near the fault zone. Kinematic indicators in the protomylonites and mylonites define left-lateral offset along the main strand of the DDMFZ on both outcrop and microstructural scale. That hydrothermal alteration, at least partly, accompanied DDMFZ deformation is indicated by microstructural arrangement of deformational structures and hydrothermal mineral species.

## Mesozoic Low-Grade Metamorphic Rocks

We divide the pre-Tertiary metamorphic rocks in the study area into two general units that are separated by the strands of the Darrington–Devils Mountain fault zone (DDMFZ): (1) the heterogeneous metamorphic rocks of the Goat Island terrane of Hopkins (1962), Whetten and others (1988), and Dragovich and others (2000c), and (2) the Helena–Haystack mélange of Tabor (1994) or Haystack terrane of Whetten and others (1980). Both units locally preserve low-temperature blueschist facies metamorphic mineral assemblages of lawsonite, aragonite, pumpellyite, and prehnite formed as a result of continental margin subduction during the Late Jurassic or Early Cretaceous. Exhumation from the subduction zone was probably accomplished by mid-Cretaceous thrusting. Both units underwent Tertiary to present fault imbrication in the DDMFZ.

### GOAT ISLAND TERRANE

The Goat Island terrane is a structurally disrupted serpentinite-matrix mélange that has lithologic and metamorphic similarities to the Lopez structural complex of the San Juan Islands (Whetten and others, 1988; Dragovich and others, 2000c, unpub. data). The Goat Island terrane contains metamorphosed mid-ocean ridge basalt (MORB), ultramafic rocks, chert, local greenstone, and metamorphosed turbidite. Sparse outcrops and Quaternary cover make contacts in the terrane difficult to observe (Plate 1). However, outcrop scale structures indicate that the Goat Island terrane occurs as imbricate slices in the DDMFZ and thus most contacts are east–west-trending, high-angle faults of the DDMFZ. Whetten and others (1988) broadly divided the terrane into metasedimentary and metavolcanic (greenstone) packages. Only metasedimentary units crop out in the study area.

Synmetamorphic static recrystallization is common in the Goat Island terrane. However, metasedimentary rocks typically contain lineated-foliated (L-S) tectonites and two or three distinct generations of folding. We relate these deformational structures to both mid-Cretaceous thrusting and later, lower strain, semiductile to brittle transpressional deformation along the DDMFZ. The structures are well displayed in the Fidalgo Complex directly northwest of the Conway quadrangle, where mid-Cretaceous thrust structures are more homogeneous and consistent in orientation and deformational overprinting effects of the DDMFZ are less pronounced or nonexistent. Within the DDMFZ, Goat Island terrane rocks are faulted and open folded with east–west fold axes. High-angle zones of cataclasite and fault breccia, 1 to 2 m thick, dissect many outcrops (Dragovich and others, 2000c, unpub data)

$KJms_g$ **Metasedimentary rocks (Cretaceous–Jurassic)**—Nonfoliated to commonly well-foliated or cleaved and typically protomylonitic metamorphosed sandstone, with lesser graywacke, siltstone or argillite (locally with a phyllitic sheen), conglomerate, minor chert, and rare marble pods and very poorly sorted conglomerate/breccia (metadiamictite). The unit is mostly well stratified; rocks vary from light to medium gray to locally reddish gray. Sandstones and conglomerates contain abundant chert and relict quartz clasts; feldspathic lithic arenite typically contains thin to thick interbeds of siltstone or slate.

Metamorphosed sandstones are composed of well-sorted, subangular to subrounded, sand-size relict clasts (80–90%) consisting mostly of monocrystalline and polycrystalline quartz, plagioclase, volcanic and sedimentary lithic clasts, and local detrital(?) chlorite and white mica; metasiltstone rip-up clasts are typical. Metamorphic minerals include quartz (1–4%), plagioclase (1–2%), muscovite (3–4%), Fe chlorite (1%), pumpellyite (0–4%), prehnite (0–1%), calcite or aragonite (1–3%), and epidote (0–3%); stilpnomelane or biotite is locally interlayered with white mica; lawsonite is present in places. Local systematic veins and stretched detrital grains are filled with pumpellyite, prehnite, and minor aragonite. Conglomerates and pebbly sandstones are thickly bedded and well stratified, are commonly interbedded with sandstone, and contain very thin or wispy interbeds of siltstone. Metamorphosed conglomerates and pebbly sandstones typically contain abundant chert clasts in a matrix that is compositionally similar to the sandstones of the complex. Metamorphosed diamictites are locally crudely bedded with sandstone and siltstone layers with pebble- to gravel-size clasts in a matrix of argillite; poor sorting may be due to mass-wasting processes such as submarine slumps (Dragovich and others, 2000c, unpub. data, this study). Metamorphosed siltstone interbeds are strongly cleaved parallel to bedding and composed of angular to subangular, silt-size ($\leq$0.01 mm) relict clasts in a dark brownish, locally graphitic, aphanitic matrix. Locally siltstones are siliceous and contain radiolarians or radiolarian ghosts.

## HELENA–HAYSTACK MÉLANGE

Most rocks of the Haystack thrust nappe of Whetten and others (1980, 1988) or the Helena–Haystack mélange (HH) of Tabor (1994) are tectonic blocks of probable Jurassic greenstone and metasedimentary rock in a serpentinite matrix. The HH is a tectonically disrupted ophiolite and contains both island arc and evolved-MORB metavolcanic and metagabbroic to metadioritic greenstones that occur as the highest thrust nappe in the Northwest Cascades System (Plate 2; Dragovich and others, 1998, 1999, 2000b; Tabor, 1994). On Scott Mountain and Devils Mountain in the Conway quadrangle, greenstone (metabasalt) is associated with serpentinite. Hydrothermal fluids injected along the DDMFZ locally completely altered the serpentinites to a resistant silica-carbonate rock called listwaenite.

Three nearly concordant U-Pb zircon age estimates obtained from intrusive greenstones north-northeast of the study area indicate a Jurassic (159–186 Ma) intrusive age for the HH (Whetten and others, 1980). Dragovich and others (1998) also obtained nearly concordant U-Pb zircon ages of 163.2 ±0.4 Ma and 162.5 ±3.5 Ma from probable Helena–Haystack mélange metagabbro northwest of the present study area. Bechtel, Inc., (1979) obtained minimum metamorphic (uplift) ages of 102 ±6 Ma and 125 ±6 Ma using K-Ar whole-rock and sericite materials, respectively, from greenstone near Devils Mountain.

Complex Helena–Haystack mélange structural relations are the result of synmetamorphic compression and structural dismemberment during subduction, late-metamorphic thrusting and exhumation (uplift), as well as transpressional deformation in the DDMFZ (Dragovich and others, 1998, 1999). Most Helena–Haystack intraformational contacts are faulted and commonly contain serpentinite derived from structural disruption of ultramafite due to Late Jurassic to Early Cretaceous mélange formation (subduction?) and (or) Cretaceous thrusting. The Helena–Haystack mélange is structurally juxtaposed against the Chuckanut Formation along fault strands of the DDMFZ, as indicated by map relations and by macroscopic and microscopic structural relations (Plate 2, cross sections A–C; Dragovich and Gilbertson, unpub. data). We infer that Helena–Haystack mélange ultramafite extends to the main strand of the DDMFZ, on the basis of magnetic anomaly geometry and structural relations (Plate 2).

$Jmv_h$ **Greenstone (Jurassic)**—Metadacitic to metabasaltic greenstone; greenish gray unweathered, orange when strongly weathered; locally contains amygdules; varies from strongly fracture-cleaved to locally massive. Sample 3E (Fig. 4, Appendix 3) is uncharacteristically siliceous and consists of small relict grains of quartz (~20%, 0.05 mm) and scattered relict plagioclase (~18 %, 0.1–0.2 mm) in a matrix of white mica (~40%), Mg-chlorite, opaque minerals, and sphene (~10%). Much of the greenstone in the study area was hydrothermally altered under static, post-metamorphic conditions that involved replacement of primary minerals and metamorphic matrix and precipitation of secondary potassium feldspar (5%), white mica (sericite), and carbonate (~7%). Although this mineralization masks the original chemistry and petrology of the greenstone by raising its $SiO_2$ content, the study area probably contains the uncommon meta-andesite to metadacitic metatuff found regionally in the Helena–Haystack mélange (Tabor, 1994; Dragovich and others, 1998).

$Ju_h$ **Ultramafite (Jurassic)**—Mostly serpentinite with local talc and tremolite-bearing serpentinite and rare allotriomorphic-granular textured, diopside-bearing, greenish gray pyroxenite in serpentinite. Serpentinite is dark greenish gray to greenish black and weathers to pale green or dark reddish yellow; very pale orange magnesite veins and bodies are common. Gradational contacts between moderately serpentinized clinopyroxenite pods and layers and surrounding thick serpentinite are the result of partial retrograde metamorphism and hydration of primary mantle rocks. Serpentinites typically grade into listwaenite (unit $Ju_{hl}$) along a 1-to-2-mm-wide transitional zone. Ultramafic rocks range from massive with spaced fracture planes to locally intensely fractured to rarely strongly foliated; most fracture or foliation surfaces are slickensided. At site 3C (Fig. 4), serpentinite contains cleaved layers of serpentine minerals and talc forming a low-temperature fabric adjacent to a north–south fault.

Serpentinite consist of serpentine-group minerals (55–90%, avg. 76%) with localized veins of chrysotile asbestos with white mica (0–5%, avg. 2%), calcite or magnesite (0–5%, avg. 2%), opaque minerals (1–10%, avg. 5%), and Fe-oxides (2–15%, avg. 8%) in a dark brown matrix (0–15%, avg. 7%) that may be the result of oxidation of associated magnetite-stained serpentinite minerals. Locally, serpentine minerals are partially replaced by magnesite and quartz (Graham, 1988). Results of our x-ray diffraction studies on serpentine minerals (Fig. 4) are most consistent with the chrysotile variety, although Graham (1988) reported that the most common serpentine mineral present is antigorite with lesser chrysotile and lizardite. However, G. Mustoe (Western Washington Univ., oral commun. to Gilbertson, 2001) indicates that it may not be possible to accurately determine variety and quantity of serpentinite species based solely on x-ray diffraction methods. Serpentinite commonly contains a few percent of clinopyroxene grains to 3 mm; elsewhere, clinopyroxene occurs as 'ghosts' and is completely converted to serpentine minerals or rarely talc.

$Ju_{hl}$ **Silica-carbonate rocks (Jurassic protolith age; mineralization post-Jurassic and probably Tertiary)**—Buff to brown to orange-brown, silica-carbonate mineralization products (listwaenites); locally contain pods of incompletely altered serpentinite and intense secondarily brecciated silica-carbonate rock; original serpentinite mesh textures locally preserved. Dominant hydrothermal minerals include microcrystalline quartz and magnesite in roughly equal amounts, with magnesite forming granular aggregates and vein swarms; magnetite occurs as an accessory mineral. Vugs 2 to 3 cm in diameter contain colorless, euhedral quartz that has overgrowths of lenticular dolomite. Brecciated silica-carbonate rock typically contains fragments (1–5 cm) in a siliceous gray matrix. Silica-carbonate rocks commonly display compositionally banded veins or replacement bands of microcrystalline or macrocrystalline quartz, microcrystalline magnesite, fibrous chalcedony, and (or) macrocrystalline dolomite. Sulfide minerals in the matrix include marcasite and pyrite. Marcasite occurs as disseminations and local granular aggregates and laths; rare pyrite occurs as euhedral cubes and pyritohedrons. Silica-carbonate rocks are often associated with Hg, Ni, Co, and W, as well as Au mineralization and are primarily composed of Mg-Fe-Ca carbonates and quartz, with accessory talc, serpentine minerals, chlorite, hematite, magnetite, pyrite, Cr mica (fuchsite) and Cr spinel. In the study area, these unusual rocks are associated with Au, Ni, and Hg geochemical anomalies (Hobbs and Pecora, 1941), but these elements are not present in economic abundances. These rocks are in fault contact with Chuckanut Formation sandstone to the south and with hydrothermally altered Helena–Haystack mélange metavolcanic and metasedimentary rocks to the east. Contacts with serpentinite are either gradational or faulted (this study; Graham, 1988).

In the study area, Helena–Haystack mélange rocks are exposed along the DDMFZ (Plates 1 and 2). Structural relations suggest that brittle to brittle-ductile deformation across the DDMFZ was accompanied by the circulation of hydrothermal fluids. Alteration is younger than the Eocene volcanic rocks and Chuckanut Formation that locally contain the silica-carbonate hydrothermal alteration. For example, a sample of silica-carbonate rock from the main strand of the DDMFZ near Devils Mountain (Fig. 4, sample 46B) is identified as altered rhyolite tuff (unit Evr) containing highly fractured quartz and plagioclase phenocrysts in a protomylonitic to mylonitic, fine-grained groundmass. Also, a distinctly mineralized and protomylonitically deformed Chuckanut Formation sandstone obtained from near the thrust fault north of the main strand of the DDMFZ contains silica-carbonate mineralization that is demonstrably syn-faulting (Fig. 4, samples 15D and 15D-1). We concur with Lovseth (1975) who suggested that hydrothermal alteration in the serpentinite is fault related and partly the result of hydrothermal circulation cells around Eocene volcanic intrusions aided by porous fault zones. For example, hydrothermal fluids were injected along the footwall of a DDMFZ thrust, altering serpentinite into a resistant, silica-carbonate rock body that forms the sharp ridge between Scott Mountain and Devils Mountain. Because of its resistance to weathering, the fault is expressed as a topographic inversion rather than as the more common deep valleys elsewhere in the study area. Our microstructural observations of samples taken along the thrust provide evidence that much of the mineralization is both synchronous with and locally continuing after thrust emplacement (Dragovich and Gilbertson, unpub. data).

$Jmc_h$ **Metasedimentary rocks (Jurassic)**—Weakly to moderately foliated slate and metamorphosed argillite, metagraywacke, and rare chert (Whetten and others, 1988). Argillite is semipelitic to locally pelitic and occurs as beds typically a few inches to a few feet thick in sandstone or as massive beds between sandstone outcrops.

## ACKNOWLEDGMENTS

This report was produced in cooperation with the U.S. Geological Survey National Cooperative Geologic Mapping Program Agreement Number 00HQAG0107. We thank Sam Johnson (USGS) for enlightening discussions, a review of the manuscript, and for providing an in-press draft of the Devils Mountain fault zone manuscript. We appreciate a review of the manuscript by Kitty Reed. We thank Richard Blakely (USGS) who kindly provided the total field magnetic anomaly maps. We appreciate the assistance of Douglas Anderson (Washington State Dept. of Transportation) with our geotechnical boring compilation. Conversations with Jim Beget (Univ. of Alaska) regarding Glacier Peak lahars were very helpful. We thank John Roozen (Washington Bulb Co. of the lower Skagit River valley) and the numerous other property owners in and around the study area for access to their property and for their cheerfulness. Thanks to George Mustoe for helpful consultations on XRD and Chuckanut fossils. Thanks also to DGER staff members Keith Ikerd, Anne Heinitz, Charles Caruthers, and Jari Roloff for cartographic support on the map, figures, correlation diagram, and explanations, Jari Roloff and Karen Meyers for editorial help, Josh Logan for a review of the manuscript, Connie Manson and Lee Walkling for assistance with references, and Diane Frederickson, Tara Salzer, and Jan Allen for clerical support.

## REFERENCES CITED

Armstrong, J. E.; Brown, W. L., 1954, Late Wisconsin marine drift and associated sediments of the lower Fraser Valley, British Columbia, Canada: Geological Society of America Bulletin, v. 65, no. 4, p. 349-364.

Armstrong, J. E.; Crandell, D. R.; Easterbrook, D. J.; Noble, J. B., 1965, Late Pleistocene stratigraphic chronology in southwestern British Columbia and northwestern Washington [abstract]: Geological Society of America Special Paper 82, p. 237.

Balzarini, M. A., 1981, Paleoecology of Everson-age glacialmarine drifts in northwestern Washington and southwestern British Columbia: University of Washington Master of Science thesis, 109 p.

Balzarini, M. A., 1983, Paleoecology of late Pleistocene glacial-marine sediments in northwestern Washington and southwestern British Columbia. *In* Molnia, B. F., editor, Glacial-marine sedimentation: Plenum Press, p. 571-592.

Bechtel, Inc., 1979, Report of geologic investigations in 1978–1979; Skagit Nuclear Power Project: Puget Sound Power and Light Company, 3 v., 3 plates

Beget, J. E., 1981, Postglacial eruption history and volcanic hazards at Glacier Peak, Washington: University of Washington Doctor of Philosophy thesis, 192 p.

Beget, J. E., 1982, Postglacial volcanic deposits at Glacier Peak, Washington, and potential hazards from future eruptions; a preliminary report: U.S. Geological Survey Open-File Report 82-830, 81 p.

Blakely, R. J.; Wells, R. E.; Weaver, C. S., 1999, Puget Sound aeromagnetic maps and data: U.S. Geological Survey Open-File Report 99-514, version 1.0 [downloaded Oct. 3, 2000 from http://geopubs.wr.usgs.gov/open-file/of99-514/].

Booth, D. B., 1987, Timing and processes of deglaciation along the southern margin of the Cordilleran ice sheet. *In* Ruddiman, W. F.; Wright, H. E., Jr., editors, North America and adjacent oceans during the last glaciation: Geological Society of America DNAG The Geology of North America, v. K-3, p. 71-90.

Booth, D. B., 1994, Glaciofluvial infilling and scour of the Puget Lowland, Washington, during ice-sheet deglaciation: Geology, v. 22, no. 8, p. 695-698.

Borden, R. K.; Troost, K. G., 2001, Late Pleistocene stratigraphy in the south-central Puget Lowland, Pierce County, Washington: Washington Division of Geology and Earth Resources Report of Investigations 33, 33 p. [Accessed July 1, 2002 at http://www.wa.gov/dnr/htdocs/ger/pdf/ri33.pdf]

Brown, E. H., 1987, Structural geology and accretionary history of the Northwest Cascades system, Washington and British Columbia: Geological Society of America Bulletin, v. 99, no. 2, p. 201-214.

Carlstad, C. A., 1992, Late Pleistocene deglaciation history at Point Partridge, central Whidbey Island, Washington: Western Washington University Master of Science thesis, 128 p.

Clague, J. J.; Saunders, I. R.; Roberts, M. C., 1988, Ice-free conditions in southwestern British Columbia at 16,000 years B.P.: Canadian Journal of Earth Sciences, v. 25, no. 6, p. 938-941.

Croll, T. C., 1980, Stratigraphy and depositional history of the Deming Sand in northwestern Washington: University of Washington Master of Science thesis, 57 p.

Danner, W. R., 1957, A stratigraphic reconnaissance in the northwestern Cascades and San Juan Islands of Washington State: University of Washington Doctor of Philosophy thesis, 3 v. [562 p.] 7 plates.

Debose, Alfonso; Klungland, M. W., 1983, Soil survey of Snohomish County area, Washington: U.S. Government Printing Office, 197 p., 59 plates.

Deeter, J. D., 1979, Quaternary geology and stratigraphy of Kitsap County, Washington: Western Washington University Master of Science thesis, 175 p., 2 plates.

Dethier, D. P.; Pessl, Fred, Jr.; Keuler, R. F.; Balzarini, M. A.; Pevear, D. R., 1995, Late Wisconsinan glaciomarine deposition and isostatic rebound, northern Puget Lowland, Washington: Geological Society of America Bulletin, v. 107, no. 11, p. 1288-1303.

Dethier, D. P.; Safioles, S. A., 1983, Map showing potential sources of sand, gravel, and quarry rock, Port Townsend quadrangle, Washington: U.S. Geological Survey Miscellaneous Investigations Series Map I-1198-B, 1 sheet, scale 1:100,000.

Dethier, D. P.; Whetten, J. T., 1980, Preliminary geologic map of the Clear Lake SW quadrangle, Skagit and Snohomish Counties, Washington: U.S. Geological Survey Open-File Report 80-825, 11 p., 2 plates, scale 1:24,000.

Dethier, D. P.; Whetten, J. T., 1981, Preliminary geologic map of the Mount Vernon 7.5-minute quadrangle, Skagit County, Washington: U.S. Geological Survey Open-File Report 81-105, 10 p., 1 plate, scale 1:24,000.

Dethier, D. P.; White, D. P.; Brookfield, C. M., 1996, Maps of the surficial geology and depth to bedrock of False Bay, Friday Harbor, Richardson, and Shaw Island 7.5-minute quadrangles, San Juan County, Washington: Washington Division of Geology and Earth Resources Open File Report 96-7, 7 p., 2 pl., scale 1:24,000.

Dickinson, W. R., 1970, Interpreting detrital modes of graywacke and arkose: Journal of Sedimentary Petrology, v. 40, no. 2, p. 695-707.

Domack, E. W., 1982, Facies of late Pleistocene glacial marine sediments on Whidbey Island, Washington: Rice University Doctor of Philosophy thesis, 393 p., 11 pl.

Domack, E. W., 1983, Facies of late Pleistocene glacial-marine sediments on Whidbey Island, Washington—An isostatic glacial-marine sequence. *In* Molnia, B. F., editor, Glacial-marine sedimentation: Plenum Press, p. 535-570.

Domack, E. W., 1984, Rhythmically bedded glaciomarine sediments on Whidbey Island, Washington: Journal of Sedimentary Petrology, v. 54, no. 2, p. 589-602.

Dragovich, J. D.; Grisamer, C. L., 1998, Quaternary stratigraphy, cross sections, and general geohydrologic potential of the Bow and Alger 7.5-minute quadrangles, western Skagit County, Washington: Washington Division of Geology and Earth Resources Open File Report 98-8, 29 p., 6 pl.

Dragovich, J. D.; McKay, D. T., Jr.; Dethier, D. P.; Beget, J. E., 2000a, Voluminous laharic inundation of the lower Skagit River valley, Washington—A product of a single large mid-Holocene Glacier Peak eruptive episode? [abstract]: Geological Society of America Abstracts with Programs, v. 32, no. 6, p. A-11.

Dragovich, J. D.; Norman, D. K.; Anderson, G., 2000b, Interpreted geologic history of the Sedro-Woolley North and Lyman 7.5-minute quadrangles, western Skagit County, Washington: Washington Division of Geology and Earth Resources Open File Report 2000-1, 71 p., 1 plate.

Dragovich, J. D.; Norman, D. K.; Grisamer, C. L.; Logan, R. L.; Anderson, Garth, 1998, Geologic map and interpreted geologic history of the Bow and Alger 7.5-minute quadrangles, western Skagit County, Washington: Washington Division of Geology and Earth Resources Open File Report 98-5, 80 p., 3 pl.

Dragovich, J. D.; Norman, D. K.; Haugerud, R. A.; Pringle, P. T., 1997, Geologic map and interpreted geologic history of the Kendall and Deming 7.5-minute quadrangles, western Whatcom County, Washington: Washington Division of Geology and Earth Resources Open File Report 97-2, 39 p., 3 pl., scale 1:24,000.

Dragovich, J. D.; Norman, D. K.; Lapen, T. J.; Anderson, Garth, 1999, Geologic map of the Sedro-Woolley North and Lyman 7.5-minute quadrangles, western Skagit County, Washington: Washington Division of Geology and Earth Resources Open File Report 99-3, 37 p., 4 pl.

Dragovich, J. D.; Troost, M. L.; Norman, D. K.; Anderson, Garth; Cass, Jason; Gilbertson, Lea A.; McKay, Donald T., Jr., 2000c, Geologic map of the Anacortes South and La Conner 7.5-minute quadrangles, Skagit and Island Counties, Washington: Washington Division of Geology and Earth Resources Open File Report 2000-6, 4 sheets, scale 1:24,000.

Easterbrook, D. J., 1962, Pleistocene geology of the northern part of the Puget Lowland, Washington: University of Washington Doctor of Philosophy thesis, 160 p.

Easterbrook, D. J., 1963a, Late Pleistocene glacial events and relative sea-level changes in the northern Puget Lowland, Washington: Geological Society of America Bulletin, v. 74, no. 12, p. 1465-1483.

Easterbrook, D. J., 1963b, Vashon glaciation and late Wisconsin relative sea-level changes in the northern part of the Puget Lowland, Washington [abstract]: Geological Society of America Special Paper 73, p. 37.

Easterbrook, D. J., 1969, Pleistocene chronology of the Puget Lowland and San Juan Islands, Washington: Geological Society of America Bulletin, v. 80, no. 11, p. 2273-2286.

Easterbrook, D. J., 1992, Advance and retreat of Cordilleran ice sheets in Washington, U.S.A.: Geographie Physique et Quaternaire, v. 46, no. 1, p. 51-68.

Easterbrook, D. J., 1994, Chronology of pre-late Wisconsin Pleistocene sediments in the Puget Lowland, Washington. *In* Lasmanis, Raymond; Cheney, E. S., convenors, Regional geology of Washington State: Washington Division of Geology and Earth Resources Bulletin 80, p. 191-206.

Easterbrook, D. J., Rutter, N. W., 1981, Amino acid ages of Pleistocene glacial and interglacial sediments in western Washington [abstract]: Geological Society of America Abstracts with Programs, v. 13, no. 7, p. 444.

Easterbrook, D. J.; Rutter, N. W., 1982, Amino acid analyses of wood and shells in development of chronology and correlation of Pleistocene sediments in the Puget Lowland, Washington [abstract]: Geological Society of America Abstracts with Programs, v. 14, no. 7, p. 480.

Evans, J. E.; Ristow, R. J., Jr., 1994, Depositional history of the southeastern outcrop belt of the Chuckanut Formation—Implications for the Darrington–Devils Mountain and Straight Creek fault zones, Washington (U.S.A.): Canadian Journal of Earth Sciences, v. 31, no. 12, p. 1727-1743.

Folk, R. L., 1980, Petrology of sedimentary rocks: Hemphill Publishing Company, 184 p.

Frederick, J. E., 1979, Map showing natural land slopes, Port Townsend quadrangle, Puget Sound region, Washington: U.S. Geological Survey Miscellaneous Investigations Series Map I-1198-A, 1 sheet, scale 1:100,000.

Frizzell, V. A., Jr., 1979, Point count data and sample locations for selected samples from Paleogene nonmarine sandstones, Washington: U.S. Geological Survey Open-File Report 79-293, 31 p., 2 plates.

Graham, D. C., 1988, Hydrothermal alteration of serpentinite associated with the Devils Mountain fault zone, Skagit County, Washington: Western Washington University Master of Science thesis, 125 p.

Hansen, H. P., Mackin, J. H., 1949, A pre-Wisconsin forest succession in the Puget Lowland, Washington: American Journal of Science, v. 247, no. 12, p. 833-855.

Hobbs, S. W.; Pecora, W. T., 1941, Nickel-gold deposit near Mount Vernon, Skagit County, Washington: U.S. Geological Survey Bulletin B093-D, p. 57-78.

Hooper, P. R.; Johnson, D. M.; Conrey, R. M., 1993, Major and trace element analyses of rocks and minerals by automated X-ray spectrometry: Washington State University Geology Department Open File Report, 36 p.

Hopkins, W. S., Jr., 1962, The geology of a portion of the Skagit delta area, Skagit County, Washington: University of British Columbia Master of Science thesis, 135 p., 1 pl.

Interpre'Tech/SeisPulse, LLC, 1996, Report of geophysical seismic reflection surveys conducted for GeoEngineers, Inc. within an area of the Skagit Valley, Washington: Interpre'Tech/SeisPulse, LLC [under contract to] GeoEngineers, 41 p.

Johnson, S. Y., 1982, Stratigraphy, sedimentology, and tectonic setting of the Eocene Chuckanut Formation, northwest Washington: University of Washington Doctor of Philosophy thesis, 221 p., 4 plates.

Johnson, S. Y., 1984a, Stratigraphy, age, and paleogeography of the Eocene Chuckanut Formation, northwest Washington: Canadian Journal of Earth Sciences, v. 21, no. 1, p. 92-106.

Johnson, S. Y., 1984b, Cyclic fluvial sedimentation in a rapidly subsiding basin, northwest Washington: Sedimentary Geology, v. 38, no. 1-4, p. 361-391.

Johnson, S. Y., 1985, Stratigraphy and sedimentology of the Eocene Chuckanut Formation on Bellingham Bay, Washington. *In* Tempelman-Kluit, Dirk, editor, Field guides to geology and mineral deposits in the southern Canadian Cordillera: Geological Association of Canada, p. 6-1–6-21.

Johnson, S. Y.; Dadisman, S. V.; Mosher, D. C.; Blakely, R. J.; Childs, J. R., 2001, Active tectonics of the Devils Mountain fault and related structures, northern Puget Lowland and eastern Strait of Juan de Fuca region, Pacific Northwest: U.S. Geological Survey Professional Paper 1643, 45 p., 2 plates.

Johnson, S. Y.; Whetten, J. T.; Naeser, C. W.; Zimmermann, R. A., 1983, Fission track ages from the Chuckanut Formation, northwest Washington [abstract]: Geological Society of America Abstracts with Programs, v. 15, no. 5, p. 393.

Keuler, R. F., 1988, Map showing coastal erosion, sediment supply, and longshore transport in the Port Townsend 30- by 60-minute quadrangle, Puget Sound region, Washington: U.S. Geological Survey Miscellaneous Investigations Series Map I-1198-E, 1 sheet, scale 1:100,000.

Klungland, M. W.; McArthur, Michael, 1989, Soil survey of Skagit County area, Washington: U.S. Department of Agriculture, Soil Conservation Service, 372 p., 67 pl., scale 1:24,000, 1:316,800.

Le Bas, M. J.; Le Maitre, R. W.; Streckeisen, A. L.; Zanettin, B., 1986, A chemical classification of volcanic rocks based on the total alkali-silica diagram: Journal of Petrology, v. 27, no. 3, p. 745-750.

Lovseth, T. P., 1975, The Devils Mountain fault zone, northwestern Washington: University of Washington Master of Science thesis, 29 p.

Marcus, K. L., 1981, The rocks of Bulson Creek—Eocene–Oligocene sedimentation and tectonics in the Lake McMurray area, Washington: Western Washington University Master of Science thesis, 84 p., 1 plate.

Mullineaux, D. R.; Waldron, H. H.; Rubin, Meyer, 1965, Stratigraphy and chronology of late interglacial and early Vashon glacial time in the Seattle area, Washington: U.S. Geological Survey Bulletin 1194-O, 10 p.

Mustoe, G. E.; Gannaway, W. L., 1997, Paleogeography and paleontology of the early Tertiary Chuckanut Formation, northwest Washington: Washington Geology, v. 25, no. 3, p. 3-18.

Myers Biodynamics, Inc., 1993, Slope stabilization and erosion control using vegetation—A manual of practice for coastal property owners: Washington Department of Ecology Publication 93-30, 42 p.

Myers Biodynamics, Inc.; Lorilla Engineering, Inc., 1995, Surface water and groundwater on coastal bluffs—A guide for Puget Sound property owners: Washington Department of Ecology Publication 95-107, 64 p.

Newcomb, R. C., 1947, Ground-water resources of Snohomish County, Washington: U.S. Geological Survey Open-File Report, 175 p., 2 plates. (Published as USGS Water-Supply Paper 1135.)

Obradovich, D. J., 1994, An updated time scale for the Cretaceous of North America [abstract]: American Association of Petroleum Geologists and Society of Economic Paleontologists and Mineralogists Annual Meeting Abstracts, p. 227.

Pessl, Fred, Jr.; Dethier, D. P.; Booth, D. B.; Minard, J. P., 1989, Surficial geologic map of the Port Townsend 30- by 60-minute quadrangle, Puget Sound region, Washington: U.S. Geological Survey Miscellaneous Investigations Series Map I-1198-F, 1 sheet, scale 1:100,000, with 13 p. text.

Pierson, T. C.; Scott, K. M., 1985, Downstream dilution of a lahar—Transition from debris flow to hyperconcentrated streamflow: Water Resources Research, v. 21, no. 10, p. 1511-1524.

Porter, S. C.; Swanson, T. W., 1998, Radiocarbon age constraints on rates of advance and retreat of the Puget lobe of the Cordilleran ice sheet during the last glaciation: Quaternary Research, v. 50, no. 3, p. 205-213.

Rau, W. W., Johnson, S. Y., 1999, Well stratigraphy and correlations, western Washington and northeastern Oregon: U.S. Geological Survey Geologic Investigation Series Map I-2621, 31 p., 3 plates.

Reiswig, K. N., 1982, Palynological differences between the Chuckanut and Huntingdon Formations, northwestern Washington: Western Washington University Master of Science thesis, 61 p.

Robertson, C. A., 1981, Petrology, sedimentology, and structure of the Chuckanut Formation, Coal Mountain, Skagit County, Washington: University of Washington Master of Science thesis, 41 p., 2 plates.

Salvador, Amos, 1985, Chronostratigraphic and geochronometric scales in COSUNA stratigraphic correlation charts of the United States: American Association of Petroleum Geologists Bulletin, v. 69, no. 2, p. 181-189.

Siegfried, R. T., 1978, Stratigraphy and chronology of raised marine terraces, Bay View Ridge, Skagit County, Washington: Western Washington University Master of Science thesis, 52 p., 1 pl.

Stoffel, K. L., 1980, Stratigraphy of pre-Vashon Quaternary sediments applied to the evaluation of a proposed major tectonic structure in Island County, Washington: Washington Division of Geology and Earth Resources Open File Report, 161 p.

Tabor, R. W., 1994, Late Mesozoic and possible early Tertiary accretion in western Washington State—The Helena–Haystack mélange and the Darrington–Devils Mountain fault zone: Geological Society of America Bulletin, v. 106, no. 2, p. 217-232, 1 pl.

Tabor, R. W.; Booth, D. B.; Vance, J. A.; Ford, A. B.; Ort, M. H., 1988, Preliminary geologic map of the Sauk River 30 by 60 minute quadrangle, Washington: U.S. Geological Survey Open-File Report 88-692, 50 p., 2 plates, 1:100,000-scale.

Thompson, Gail, 1978, Prehistoric settlement changes in the southern northwest coast—A functional approach: University of Washington Doctor of Philosophy thesis, 252 p.

Varnes, D. J., 1978, Slope movement types and processes. *In* Schuster, R. L.; Krizek, R. J., editors, Landslides—Analysis and control: National Research Council Transportation Research Board Special Report 176, p. 11-33.

Washington Department of Ecology, 1978, Coastal zone atlas of Washington; volume 1, Whatcom County: Washington Department of Ecology, 1 v., maps, scale 1:24,000.

Whetten, J. T.; Carroll, P. I.; Gower, H. D.; Brown, E. H.; Pessl, Fred, Jr., 1988, Bedrock geologic map of the Port Townsend 30- by 60-minute quadrangle, Puget Sound region, Washington: U.S. Geological Survey Miscellaneous Investigations Series Map I-1198-G, 1 sheet, scale 1:100,000.

Whetten, J. T.; Dethier, D. P.; Carroll, P. R., 1979, Preliminary geologic map of the Clear Lake NE quadrangle, Skagit County, Washington: U.S. Geological Survey Open-File Report 79-1468, 10 p., 2 plates.

Whetten, J. T.; Zartman, R. E.; Blakely, R. J.; Jones, D. L., 1980, Allochthonous Jurassic ophiolite in northwest Washington: Geological Society of America Bulletin, v. 91, no. 6, p. I 359-I 368.

Zanettin, B., 1984, Proposed new chemical classification of volcanic rocks: Episodes, v. 7, no. 4, p. 19-20. ■

# CALIBRATION OF RADIOCARBON AGE TO CALENDAR YEARS

(Variables: C13/C12=-28.7:lab. mult=1)

**Laboratory number:** **150023**

**Conventional radiocarbon age:** **2630±60 BP**

**2 Sigma calibrated result: (95% probability)** **Cal BC 900 to 770 (Cal BP 2850 to 2720)**

Intercept data

Intercept of radiocarbon age with calibration curve: Cal BC 800 (Cal BP 2760)

1 Sigma calibrated result: (68% probability) Cal BC 820 to 790 (Cal BP 2780 to 2740)

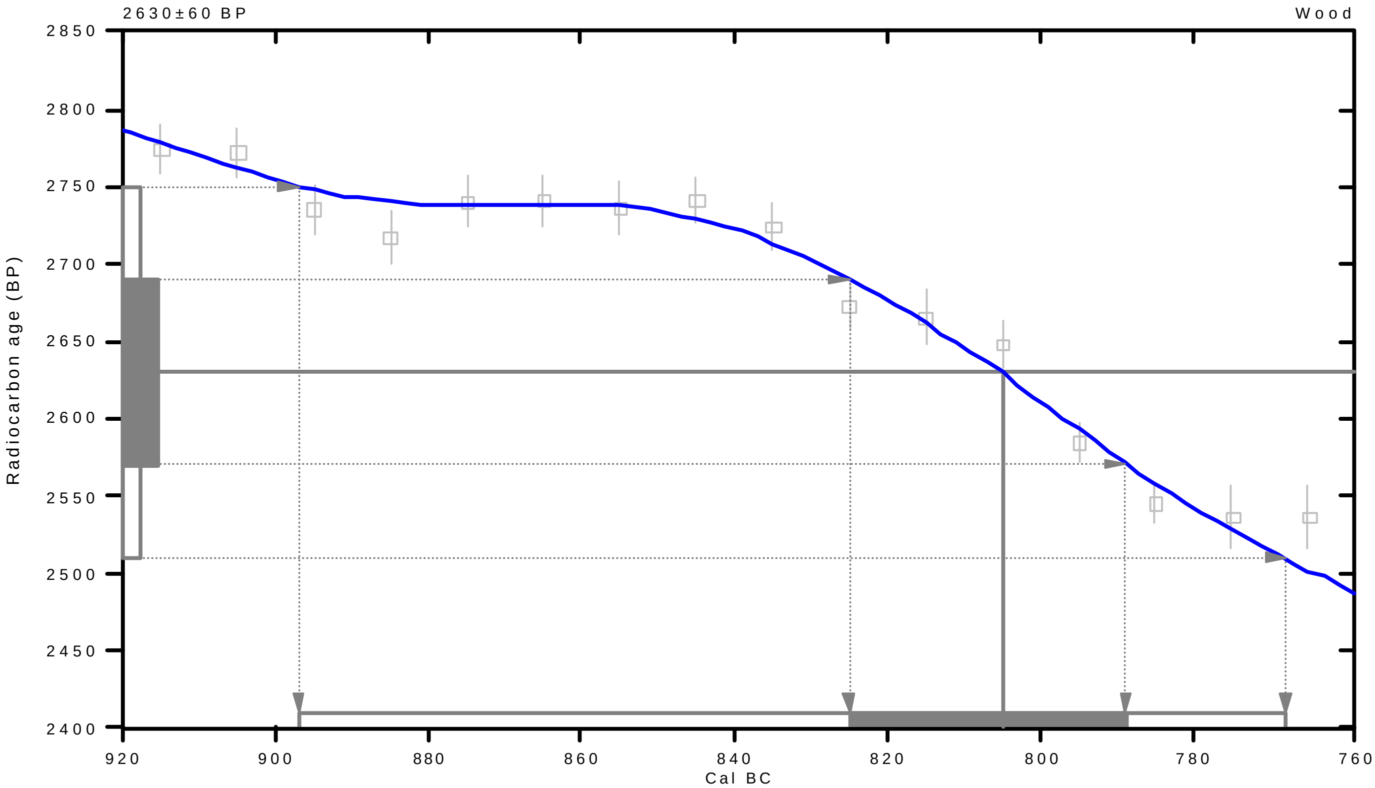


References:

***Database used***

***Calibration Database***
***Editorial Comment***
*Stuiver, M., van der Plicht, H., 1998, Radiocarbon 40(3), pxii-xiii*
***INTCAL98 Radiocarbon Age Calibration***
*Stuiver, M., et. al., 1998, Radiocarbon 40(3), p1041-1083*
***Mathematics***
***A Simplified Approach to Calibrating C14 Dates***
*Talma, A. S., Vogel, J. C., 1993, Radiocarbon 35(2), p317-322*

**Beta Analytic Inc.**

*4985 SW 74 Court, Miami, Florida 33155 USA • Tel: (305) 667 5167 • Fax: (305) 663 0964 • E-Mail: beta@radiocarbon.com*

# CALIBRATION OF RADIOCARBON AGE TO CALENDAR YEARS

(Variables: C13/C12=-27.8:lab. mult=1)

**Laboratory number:** **150026**

**Conventional radiocarbon age:** **820±70 BP**

**2 Sigma calibrated result: (95% probability)** **Cal AD 1030 to 1290 (Cal BP 920 to 660)**

Intercept data

Intercept of radiocarbon age with calibration curve: Cal AD 1230 (Cal BP 720)

1 Sigma calibrated result: (68% probability) Cal AD 1170 to 1270 (Cal BP 780 to 680)

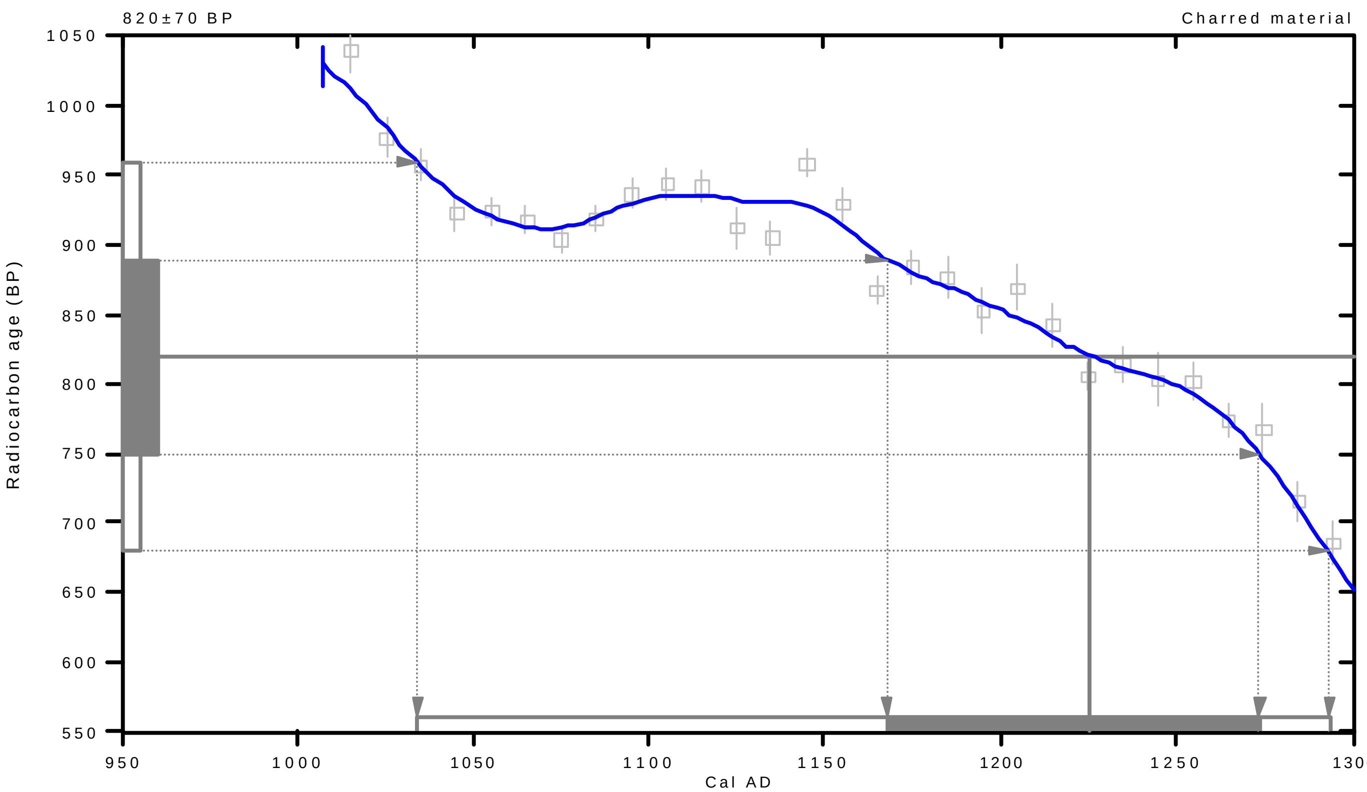



References:

***Database used***

***Calibration Database***
***Editorial Comment***
*Stuiver, M., van der Plicht, H., 1998, Radiocarbon 40(3), pxii-xiii*
***INTCAL98 Radiocarbon Age Calibration***
*Stuiver, M., et. al., 1998, Radiocarbon 40(3), p1041-1083*
***Mathematics***
***A Simplified Approach to Calibrating C14 Dates***
*Talma, A. S., Vogel, J. C., 1993, Radiocarbon 35(2), p317-322*



**Beta Analytic Inc.**

*4985 SW 74 Court, Miami, Florida 33155 USA • Tel: (305) 667 5167 • Fax: (305) 663 0964 • E-Mail: beta@radiocarbon.com*

# CALIBRATION OF RADIOCARBON AGE TO CALENDAR YEARS

(Variables: C13/C12=-27:lab. mult=1)

**Laboratory number:** **Beta-150029**

**Conventional radiocarbon age:** **4090±80 BP**

**2 Sigma calibrated result: (95% probability)** **Cal BC 2890 to 2460 (Cal BP 4840 to 4410)**

Intercept data

Intercept of radiocarbon age with calibration curve: Cal BC 2600 (Cal BP 4560)

1 Sigma calibrated results: (68% probability)
Cal BC 2860 to 2800 (Cal BP 4810 to 4750) and
Cal BC 2760 to 2550 (Cal BP 4710 to 4500) and
Cal BC 2540 to 2490 (Cal BP 4480 to 4440)

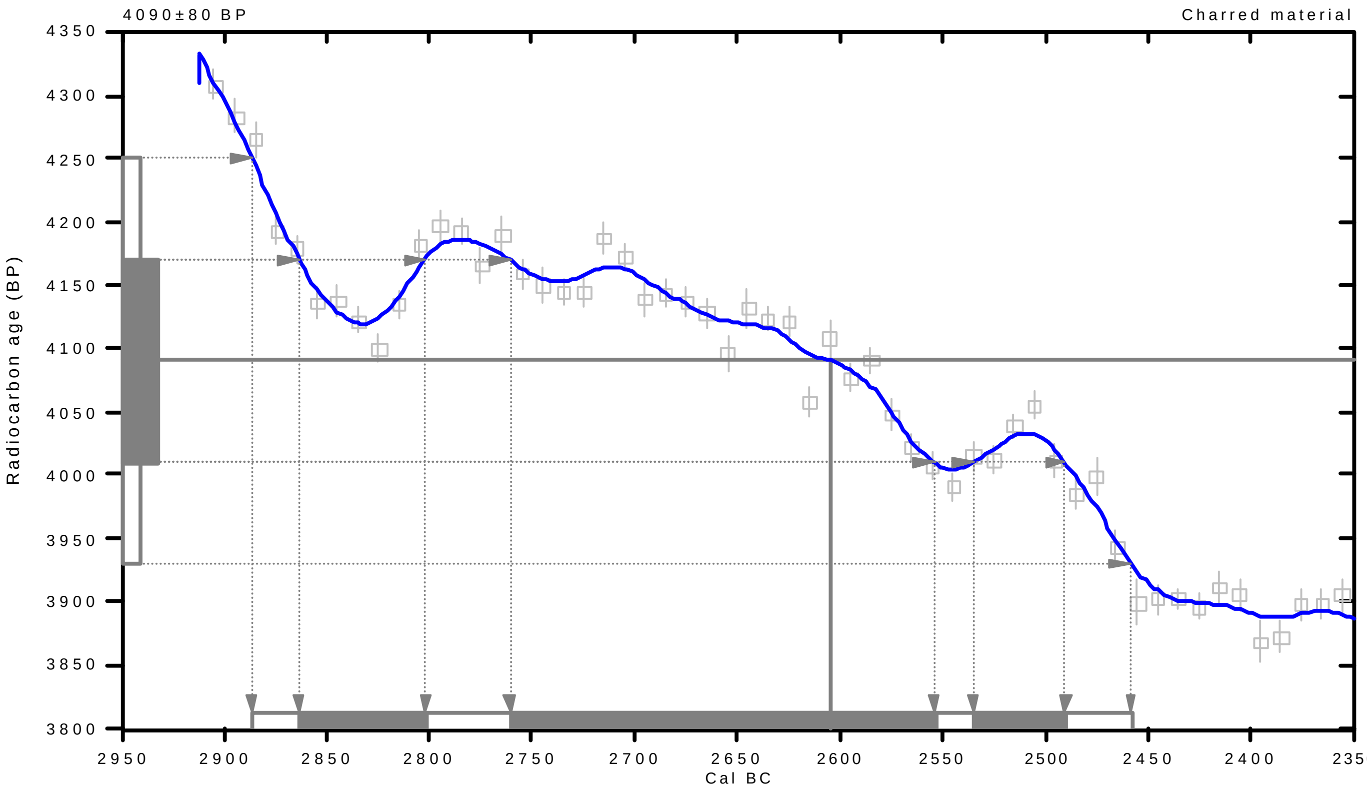



References:

***Database used***

***Calibration Database***
***Editorial Comment***
*Stuiver, M., van der Plicht, H., 1998, Radiocarbon 40(3), pxii-xiii*
***INTCAL98 Radiocarbon Age Calibration***
*Stuiver, M., et. al., 1998, Radiocarbon 40(3), p1041-1083*
***Mathematics***
***A Simplified Approach to Calibrating C14 Dates***
*Talma, A. S., Vogel, J. C., 1993, Radiocarbon 35(2), p317-322*



**Beta Analytic Inc.**

*4985 SW 74 Court, Miami, Florida 33155 USA • Tel: (305) 667 5167 • Fax: (305) 663 0964 • E-Mail: beta@radiocarbon.com*

# Appendix 1. Radiocarbon ages, this study

$^{14}C$ analyses performed by Beta Analytic, Inc. (Miami, Fla.). Sample locations are shown on Figure 4. Dates are reported as radiocarbon years before present (yr B.P.)(present = A.D. 1950). We report the uncalibrated ages in the text. The quoted results are calibrated to calendar years in the graphs below. By international convention, the modern reference standard was 95 percent of the $^{14}C$ content of the National Bureau of Standards' oxalic acid and calculated using the Libby $^{14}C$ half-life (5,568 years). Quoted errors represent 1 standard deviation (68% probability) and are based on combined measurements of the sample, background, and modern reference standards. Measured $^{13}C/^{12}C$ ratios were calculated relative to the PDB-1 international standard, and the radiocarbon years before present ages were normalized to -25 per mil.

### Sample 5G: Unit Qp

Wood (4.7 gm) from sticks obtained from 5.3 ft (1.6 m) below surface from test pit. Dated stick is 2 in. (6 cm) long and 1.1 in. (3 cm) in diameter and contains some preserved bark. Wood occurs in silty clay layer containing scattered wood fragments. The silty clay layer contains gravel seams and is overlain by 4 ft (1.2 m) of peat. Wood sampled 1.3 ft (0.4 m) below peat/silty clay contact. Silty clay layer is probably lacustrine/swamp sediment formed in this flat area.

| Measured $^{14}C$ age (yr B.P.) | $^{13}C/^{12}C$ ratio | Conventional $^{14}C$ age (yr B.P.) |
|---|---|---|
| 2,690 ± 60 | -28.7‰ | 2,630 ±60 |

Beta-150023 (see p. 25)
Analysis: Radiometric-Standard delivery
Material (pretreatment): wood (acid/alkali/acid)
Location: Fig. 4, site 5G; east-central Conway quadrangle

### Sample 26H: Unit Qn

Charred wood (14 gm) found 3.0 ft (0.9 m) below surface in a ditch in Skagit River sands and silts. Wood is from a 7 in. (5 cm) organic rich layer; this layer is overlain by 2.8 ft (0.9 m) of gray organic silt and underlain by non-organic gray silt that grades to fine sand. Surface contains a thin, silty organic topsoil. Sample probably approximately dates onset of terrestrial (non-estuarine) conditions at the site.

| Measured $^{14}C$ age (yr B.P.) | $^{13}C/^{12}C$ ratio | Conventional $^{14}C$ age (yr B.P.) |
|---|---|---|
| 870 ±70 | -27.8‰ | 820 ±70 |

Beta-150026 (see p. 26)
Analysis: Radiometric-Standard delivery
Material (pretreatment): charred material (acid/alkali/acid)
Location: Fig. 4, site 26H; west-central Conway quadrangle near South Fork Skagit River

### Sample 59I: Unit Qp

Charcoal (0.25 gm) in a dark brown paleosol or organic silt. Paleosol occurs below buff-tan to light orange-tan ash (reworked?) of unknown age; paleosol overlies silty clay with scattered pebbles (glaciomarine drift; unit $Qgdm_{ed}$) which overlies sandy gravel outwash of probable near-ice depositional origin as indicated by contorted bedding. Located in a new landscaping pond exposure on Bulson Road at an elevation of about 320 ft (98 m). This new exposure is about 10 ft (3 m) deep and appears to be in an area that is a long-lived swampy depression with localized peat deposition formed on low-permeability glaciomarine drift.

| Measured $^{14}C$ age (yr B.P.) | $^{13}C/^{12}C$ ratio | Conventional $^{14}C$ age (yr B.P.) |
|---|---|---|
| 4,120 ±80 | -27‰ | 4,090 ±80 |

Beta-150029 (see p. 27)
Analysis: AMS-Standard delivery
Material (pretreatment): charred material (acid/alkali/acid)
Location: Fig. 4, site 59I; central Conway quadrangle

# Appendix 2. Point-count and QFL data, this study

Thin sections of well-sorted, fine- to medium-grained unconsolidated sands (0.1–2 mm diameter grains) from various Quaternary geologic units and one sandstone were point-counted every 1 $mm^2$ (394–520 points) using a petrographic microscope. See Figure 4 for sample locations. These data were used to interpret the general provenance of the sand. See Appendix 4 for a discussion of the Glacier Peak provenance of the microlitic dacite in outwash sands.

### TABLE A. POINT-COUNT SAMPLE DESCRIPTIONS

| Sample | Unit | Location | Point count notes and general interpretation |
|---|---|---|---|
| SR | $Qa_s$ sand | Skagit River, northernmost Conway quadrangle | Main constituents include microlitic volcanic fragments, monocrystalline quartz, plagioclase, and undivided metamorphic and igneous lithic clasts. Other detrital grains include hypersthene, hornblende, and clinopyroxene. Significant amounts of dacite fragments are present and contain hornblende and some clinopyroxene. Reworked lahar appears to be a significant component of the alluvium deposited on this point bar. |
| 30I | Qn sand | northwest edge of Utsalady quadrangle | Main constituents include microlitic volcanic fragments (dacite), monocrystalline quartz, and plagioclase; lesser amounts of potassium feldspar, hornblende, hypersthene, quartz-mica tectonite, chert, and epidote. Other lithic clasts include serpentinite, greenstone, greenschist, sandstone, and granitics. Typical Skagit delta tidal flats sand. Reworked lahar appears to be a significant component of the tidal flats. |
| 41D | Qvl? sand | adjacent to Highway 534, northwest Conway quadrangle | Main constituents include microlitic volcanic fragments, monocrystalline quartz, and plagioclase; significant amounts of hypersthene and hornblende; lesser polycrystalline quartz, white mica, granitic lithic clasts, and greenstone. Plagioclase is subangular, and most grains have oscillatory zoning. On the basis of its angularity and high percentage of dacitic microlitic volcanic fragments and detrital mineral content (plagioclase, hypersthene, hornblende and augite), this sand is inferred to be a lahar runout or hyperconcentrated flood deposit. |
| 1D | $Qgom_e$ sand | gravel quarry, southeast Conway quadrangle | Main constituents include monocrystalline quartz, plagioclase, microlitic volcanic fragments, undifferentiated polycrystalline quartz, sedimentary lithic clasts, undivided metamorphic lithic clasts, and quartzo-feldspathic lithic clasts; lesser amounts of hypersthene, potassium feldspar, serpentinite, and greenstone. This outwash contains significant dacitic volcanic fragments, augite, hornblende, hypersthene, volcanic quartz, and plagioclase, and thus reflects a distinct but partial Glacier Peak volcanic provenance. |
| 9R | $Qgom_e$ sand | Frontage Road near I-5 on-ramp, central Conway quadrangle | Main constituents include monocrystalline quartz, plagioclase, sedimentary lithic clasts, quartzo-feldspathic lithic clasts, and undifferentiated polycrystalline quartz; significant chert, undifferentiated quartz-mica tectonite, undivided metamorphic lithic clasts, potassium feldspar, greenstone, and microlitic volcanic lithics, and undivided volcanic fragments; lesser amounts of hypersthene, clinopyroxene, and epidote. Presence of potassium feldspar, greenstone, serpentinite, and sedimentary lithic clasts suggests sediments were partially derived from erosion of the bedrock hills in the northeast part of the Conway quadrangle. |
| 29A | $Qga_v$ sand | Brown Point, southwest Utsalady quadrangle | Main constituents include monocrystalline quartz, plagioclase, chert, quartz-mica tectonite, polycrystalline quartz, greenstone, quartz-feldspar metamorphic lithic clasts, and undivided sedimentary and metamorphic lithic clasts; lesser amounts of potassium feldspar, microlitic volcanic fragments, quartzo-feldspathic lithic clasts, clinopyroxene, hornblende, serpentinite, olivine, greenstone, epidote, and possible hypersthene. Clasts are medium-grained, well-sorted, and subrounded. Advance outwash is polymict and has a probable northern derivation from Fidalgo Island to the Coast Mountains of British Columbia. |
| 29Fb | $Qc_o$ sand | Utsalady Point, far southwest corner Utsalady quadrangle | Main constituents include monocrystalline quartz, plagioclase, microlitic volcanic fragments, quartzo-feldspathic lithic clasts, sedimentary lithic clasts, and undivided metamorphic lithic clasts; also contains quartz-mica tectonite, chert, undifferentiated polycrystalline quartz, potassium feldspar, greenstone, and undifferentiated volcanic lithic clasts; lesser clinopyroxene, orthopyroxene, hornblende, biotite, greenschist, hypersthene, granitic lithic clasts, and epidote. Probable polymictic ancient Skagit River alluvium; occurrence of hypersthene and microlitic volcanic fragments suggests partial Glacier Peak volcanic provenance, comparable to point-counted Olympia sand samples from Whidbey Island northwest of the study area and Skagit River alluvium sampled across much of the lower Skagit River valley (Dragovich and others, unpub. data). |
| 15A-1 | $Ec_b$ arkosic sandstone | Devils Mountain, northeast Conway quadrangle | Main constituents include monocrystalline quartz, plagioclase, chert, and potassium feldspar. Contains significant quartz-mica tectonite, quartzo-feldspathic lithic clasts, and undifferentiated volcanic lithics; lesser undifferentiated polycrystalline quartz, microlitic volcanic lithic clasts, white mica, biotite, sedimentary lithic clasts, and garnet; significant iron oxide. Likely lower Chuckanut Formation (note potassium feldspar abundance). |

## TABLE B. POINT COUNT DATA (PERCENT)

**, the quartzo-feldspathic lithic clasts (undivided) category includes mostly granitic lithic clasts, but also locally includes probable sandstone or other quartz- and feldspar-rich fragments

| Geologic Unit | $Qa_s$ | Qn | Qvl? | $Qgom_e$ | $Qgom_e$ | $Qga_v$ | $Qc_o$ | $Ec_b$ |
|---|---|---|---|---|---|---|---|---|
| **Sample Number** | **SR** | **30I** | **41D** | **1D** | **9R** | **29A** | **29Fb** | **15A-1** |
| monocrystalline quartz | 5.4 | 13.4 | 4.7 | 19.5 | 16.8 | 14.1 | 18.8 | 39.6 |
| quartz-mica tectonite (QMT) | 4.8 | 2.4 | 0.6 | 2.5 | 5.1 | 5.1 | 4.5 | 4.9 |
| polycrystalline quartz, undivided (PQ) | 2.9 | 3.5 | 0.9 | 6.1 | 10.4 | 6.5 | 3.1 | 0.6 |
| chert | 0.4 | 0.4 | 0.2 | 0.2 | 5.6 | 6.0 | 3.8 | 7.9 |
| plagioclase | 9.2 | 15.0 | 19.0 | 21.5 | 12.4 | 13.4 | 19.6 | 16.9 |
| potassium feldspar | 0.6 | 0.4 | 0.4 | 1.6 | 2.8 | 3.0 | 2.9 | 7.1 |
| microlitic volcanic lithic clasts (dacite) | 35.4 | 37.7 | 51.0 | 13.2 | 3.3 | 3.0 | 8.3 | 0.4 |
| volcanic lithic clasts, undivided (volcanics) | 5.6 | 3.5 | 1.5 | 1.3 | 4.1 | 3.2 | 2.7 | 3.0 |
| sedimentary lithic clasts, undivided | 5.0 | 6.2 | 3.0 | 9.0 | 10.9 | 8.3 | 8.9 | 0.2 |
| metamorphic lithic clasts, undivided | 8.3 | 3.7 | 2.8 | 5.2 | 5.6 | 7.9 | 6.9 | 0.2 |
| greenstone | 3.8 | 0.7 | 1.1 | 3.6 | 3.3 | 5.5 | 4.7 | 0.0 |
| quartzo-feldspathic lithic clasts, undivided ** | 6.9 | 3.5 | 2.8 | 7.2 | 10.7 | 20.8 | 11.2 | 4.7 |
| phyllite | 1.9 | 0.9 | 0.2 | 0.0 | 0.8 | 0.0 | 0.0 | 0.0 |
| greenschist | 0.4 | 1.3 | 0.0 | 0.4 | 0.3 | 0.2 | 0.4 | 0.0 |
| carbonate minerals | 0.0 | 0.2 | 0.0 | 0.0 | 0.0 | 0.5 | 0.0 | 0.0 |
| chlorite | 0.4 | 0.2 | 0.2 | 0.2 | 0.3 | 0.0 | 0.2 | 0.0 |
| serpentinite | 0.8 | 0.4 | 0.6 | 2.9 | 1.5 | 0.5 | 0.7 | 0.0 |
| garnet | 0.4 | 0.2 | 0.6 | 0.7 | 0.5 | 0.2 | 0.7 | 1.0 |
| hypersthene | 2.1 | 0.9 | 3.8 | 2.2 | 1.0 | 0.0 | 0.0 | 0.0 |
| clinopyroxene (including augite) | 1.3 | 0.9 | 0.4 | 0.0 | 1.5 | 0.7 | 0.4 | 0.0 |
| orthopyroxene | 0.0 | 0.4 | 0.0 | 0.0 | 0.8 | 0.0 | 0.2 | 0.0 |
| actinolite | 0.0 | 0.0 | 0.2 | 0.2 | 0.3 | 0.0 | 0.0 | 0.0 |
| hornblende | 1.3 | 1.5 | 3.4 | 0.2 | 0.3 | 0.2 | 0.9 | 0.0 |
| biotite | 0.2 | 1.1 | 0.6 | 0.2 | 0.8 | 0.0 | 0.7 | 0.4 |
| white mica | 0.4 | 0.4 | 0.2 | 0.2 | 0.0 | 0.0 | 0.0 | 1.2 |
| opaque minerals | 1.9 | 0.0 | 0.6 | 1.1 | 1.0 | 0.0 | 0.0 | 0.2 |
| sphene | 0.0 | 0.0 | 0.2 | 0.0 | 0.0 | 0.0 | 0.0 | 0.0 |
| epidote | 0.6 | 0.7 | 0.4 | 0.4 | 0.3 | 0.5 | 0.2 | 0.0 |
| olivine | 0.0 | 0.0 | 0.0 | 0.0 | 0.0 | 0.5 | 0.2 | 0.0 |
| iron oxide | 0.0 | 0.2 | 0.4 | 0.2 | 0.0 | 0.0 | 0.0 | 6.7 |
| Total (percent) | 100.0 | 100.0 | 100.0 | 100.0 | 100.0 | 100.0 | 100.0 | 100.0 |
| Total points counted | 520 | 454 | 469 | 446 | 394 | 433 | 448 | 492 |

## TABLE C. QFL data and related data (percent)

Q, quartz; F, feldspar; L, lithic clasts (see Table B for other abbreviations)

| **Geologic Unit** | **$Qa_s$** | **Qn** | **Qvl?** | **$Qgom_e$** | **$Qgom_e$** | **$Qga_v$** | **$Qc_o$** | **$Ec_b$** |
|---|---|---|---|---|---|---|---|---|
| **Sample number** | **SR** | **30I** | **41D** | **1D** | **9R** | **29A** | **29Fb** | **15A-1** |
| Q (all quartz clasts with chert) | 14.9 | 21.4 | 7.3 | 31.0 | 41.2 | 32.6 | 31.5 | 62.6 |
| F | 10.8 | 16.6 | 22.0 | 25.3 | 16.6 | 16.9 | 23.5 | 27.6 |
| L (without chert) | 74.3 | 62.0 | 70.7 | 43.7 | 42.3 | 50.5 | 45.0 | 9.8 |
| SUM | 100.0 | 100.0 | 100.0 | 100.0 | 100.0 | 100.0 | 100.0 | 100.0 |
| Q (all quartz clasts without chert) | 14.4 | 20.9 | 7.0 | 30.7 | 35.1 | 26.4 | 27.5 | 53.5 |
| F | 10.8 | 16.6 | 22.0 | 25.3 | 16.6 | 16.9 | 23.5 | 27.6 |
| L (with chert) | 74.7 | 62.5 | 70.9 | 44.0 | 48.3 | 56.7 | 49.0 | 18.9 |
| SUM | 100.0 | 100.0 | 100.0 | 100.0 | 100.0 | 100.0 | 100.0 | 100.0 |
| Q (chert+PQ+QMT) | 13.9 | 10.2 | 2.3 | 19.5 | 51.6 | 47.2 | 27.1 | 42.2 |
| plagioclase | 15.8 | 23.9 | 25.9 | 48.0 | 30.4 | 36.0 | 46.8 | 48.0 |
| Total volcanic lithic clasts | 70.3 | 65.8 | 71.7 | 32.5 | 18.0 | 16.8 | 26.1 | 9.8 |
| SUM | 100.0 | 100.0 | 100.0 | 100.0 | 100.0 | 100.0 | 100.0 | 100.0 |
| volcanic lithics/Q+F+L | 45.2 | 44.4 | 59.6 | 16.0 | 8.0 | 6.4 | 11.4 | 4.0 |
| chert/Q+F+L | 0.4 | 0.5 | 0.2 | 0.2 | 6.1 | 6.2 | 4.0 | 9.1 |

# Appendix 3. Major and minor element geochemical analyses, this study

Tables containing sample descriptions, unnormalized, and trace element geochemical data. Sample locations are shown on Figure 4. All analyses are Rigaku x-ray fluorescence (XRF) and ICP analyses performed at the Geology Department, Washington State University, Pullman, WA 99164, under the direction of Diane Johnson. Major elements are normalized on a volatile-free basis, with total Fe expressed as FeO. A 'rerun' after a sample number indicates a rerun of a duplicate bead made from the same rock powder; avg., indicates average of two runs. A description of the method and estimates of the precision and accuracy are given in Hooper and others (1993). DDMFZ, Darrington–Devils Mountain fault zone. See Appendix 4 for a brief discussion of the petrologic, petrographic, and geochemical evidence for Glacier Peak volcanic detritus in recessional glacial outwash.

## TABLE A. GEOCHEMICAL SAMPLE DESCRIPTIONS

| Sample | Location | Unit | Notes |
|---|---|---|---|
| DACITE CLAST IN SAND AND GRAVEL OF MODERN SKAGIT RIVER ALLUVIUM ON POINT BAR | | | |
| SR | Skagit River, northernmost Conway quadrangle | dacite clast in $Qa_s$ | Dacite clast from Skagit River point bar gravel. Clasts up to 1.2 in. (3 cm) in diameter constitute about 20 percent of the gravel fraction. Dacite clasts are mostly homogeneous in composition and represent alluvium derived from reworked Glacier Peak lahar deposits mapped upvalley by Dragovich and others (2000c). |
| DACITE CLASTS IN EVERSON INTERSTADE RECESSIONAL OUTWASH | | | |
| 1D-1 | gravel quarry, southeast Conway quadrangle | dacite clast in $Qgom_e$ | Well-rounded, gray dacite clast in glacial outwash; glomerocrystic; porphyritic, containing phenocrysts of plagioclase, hypersthene, clinopyroxene (augite), and hornblende in glassy matrix with microlites of plagioclase that are subhedral to euhedral with normal and oscillatory zoning. Hypersthene is subhedral to euhedral and may be rimmed by augite. Presence of augite, hypersthene, and hornblende suggests Glacier Peak provenance. |
| 2B | gravel quarry, southeast Conway quadrangle | dacite clast in $Qgom_e$ | Well-rounded, light gray to gray dacite clast in glacial outwash; porphyritic, contains phenocrysts of plagioclase, orthopyroxene (hypersthene), clinopyroxene (augite), hornblende (possibly oxyhornblende), and minor olivine in a glassy matrix with microlites of plagioclase and glomerocrysts. Plagioclase is subhedral to euhedral with normal and oscillatory zoning; hornblende and hypersthene are subhedral to euhedral; augite commonly rims hornblende and hypersthene. Phenocryst type data of Beget (1981), combined with our data, suggest dacite clasts are outwash derived from the White Chuck assemblage (Beget, 1981) or possibly an older dacitic Glacier Peak source with similar mineralogy. |
| 2B-2 | gravel quarry, southeast Conway quadrangle | dacite clast in $Qgom_e$ | Dacite clast in outwash; no petrographic data. |
| HELENA–HAYSTACK GREENSTONE; NORTHWEST CASCADE SYSTEM | | | |
| 3e | north-central Conway quadrangle | $Jmv_h$ greenstone | Greenish-gray, mineralized, siliceous, metatuffaceous greenstone with abundant quartz crystals and scattered plagioclase phenocrysts. Contains small phenocrysts (~0.05 mm) of plagioclase and monocrystalline quartz; most grains have undergone static mineralization with replacement by white mica and carbonate and resultant diffuse grain boundaries. Rock exhibits a slight tectonic grain shape fabric and optical alignment. Some grains of white mica are aligned along weak cleavage related to Tertiary offset along DDMFZ or older metamorphism. Most mineralization is post-tectonic. |
| EOCENE SILICIC VOLCANIC ROCKS | | | |
| 36F | north central Conway quadrangle | Evr andesite | Dark gray vesicular andesite. Contains microlites of plagioclase and clinopyroxene in a fine-grained, dark glassy matrix. Plagioclase is acicular and euhedral; matrix is dark due to epidote-like mineral and dark inclusions in glass; minor carbonate, iron oxide, and epidote mineralization. Plagioclase is weakly sauseritized. Veins and vesicles are filled by carbonate, chlorite, opaque minerals, and epidote-like mineral. There are Fe-oxide weathering products along conspicuous fractures |
| 53P | Johnson Creek fault zone, northcentral Conway quadrangle | Evr andesite | Phenocrysts of plagioclase and calcic-clinopyroxene in microlitic glassy matrix. Plagioclase occurs mostly as subhedral to anhedral ragged grains in static orientation; commonly sericitized. Clinopyroxene converted to chlorite, biotite, and white mica. Also contains interstitial quartz and disseminated opaque minerals; probable vesicles filled with carbonate. Hydrothermal alteration products include sphene and calcite. There are late veins of calcite and biotite. Textural relations suggest flow or hypabyssal andesitic intrusive. |
| 36G | northcentral Conway quadrangle | Evr rhyolite | Light gray, crystal vitric rhyolitic tuff with phenocrysts of quartz, plagioclase, and volcanic lithics in a eutaxitic, cryptocrystalline, yellowish-brownish glassy matrix. Contains squashed vesicles and pumice fragments. Glass is clear; quartz is euhedral to subhedral, embayed and resorbed; plagioclase is euhedral; flow banding is present. There are a few lithic fragments of rhyolite. |
| 40G | northcentral Conway quadrangle, Johnson Creek | Evr andesite | Plagioclase microlites in a tan to yellow glassy matrix with spherulites. Plagioclase occurs as statically aligned microlitic needles. Vesicles are are aligned and filled with quartz and opal. Flow or maybe tuff? |

## TABLE B. MAJOR ELEMENT GEOCHEMICAL DATA, UNNORMALIZED (WEIGHT PERCENT)

(see Table A for sample descriptions)

| Sample | $SiO_2$ | $Al_2O_3$ | $TiO_2$ | FeO | MnO | CaO | MgO | $K_2O$ | $Na_2O$ | $P_2O_5$ | Total |
|---|---|---|---|---|---|---|---|---|---|---|---|
| DACITE CLAST IN SAND AND GRAVEL OF MODERN SKAGIT RIVER ALLUVIUM | | | | | | | | | | | |
| SR | 64.10 | 16.14 | 0.570 | 3.95 | 0.081 | 4.69 | 2.34 | 2.13 | 3.97 | 0.147 | 98.12 |
| DACITE CLASTS IN EVERSON INTERSTADE RECESSIONAL OUTWASH | | | | | | | | | | | |
| 1D-1 | 63.43 | 16.58 | 0.622 | 4.13 | 0.080 | 4.99 | 2.35 | 2.22 | 4.00 | 0.154 | 98.56 |
| 2B | 61.91 | 17.09 | 0.674 | 4.48 | 0.086 | 5.48 | 2.57 | 2.00 | 3.93 | 0.152 | 98.37 |
| 2B-2 | 61.81 | 16.91 | 0.731 | 4.98 | 0.094 | 5.70 | 3.10 | 1.81 | 4.06 | 0.157 | 99.35 |
| HELENA–HAYSTACK GREENSTONE; NORTHWEST CASCADE SYSTEM | | | | | | | | | | | |
| 3E | 69.79 | 14.30 | 0.425 | 3.05 | 0.110 | 2.36 | 1.22 | 2.68 | 3.20 | 0.130 | 97.27 |
| EOCENE SILICIC VOLCANIC ROCKS | | | | | | | | | | | |
| 36F | 58.51 | 13.81 | 1.502 | 10.62 | 0.264 | 5.88 | 1.52 | 1.22 | 3.67 | 0.513 | 97.51 |
| 36F (rerun) | 58.41 | 13.84 | 1.511 | 10.36 | 0.264 | 5.91 | 1.59 | 1.22 | 3.63 | 0.521 | 97.26 |
| 53P | 58.33 | 16.34 | 0.816 | 5.38 | 0.135 | 3.68 | 6.57 | 1.20 | 3.91 | 0.236 | 96.60 |
| 36G | 76.76 | 11.97 | 0.242 | 1.08 | 0.008 | 0.43 | 0.23 | 5.15 | 1.43 | 0.025 | 97.33 |
| 40G | 73.46 | 12.60 | 0.189 | 1.84 | 0.011 | 1.33 | 0.26 | 2.62 | 2.60 | 0.009 | 94.92 |

### Trace Elements (ppm)

| Sample | La | Ce | Pr | Nd | Sm | Eu | Gd | Tb | Dy | Ho | Er | Tm | Yb | Lu |
|---|---|---|---|---|---|---|---|---|---|---|---|---|---|---|
| DACITE CLAST IN SAND AND GRAVEL OF MODERN SKAGIT RIVER ALLUVIUM | | | | | | | | | | | | | | |
| SR | 15.97 | 31.10 | 3.59 | 14.16 | 3.24 | 0.94 | 2.96 | 0.47 | 2.89 | 0.58 | 1.64 | 0.24 | 1.55 | 0.25 |
| DACITE CLASTS IN EVERSON INTERSTADE RECESSIONAL OUTWASH | | | | | | | | | | | | | | |
| 1D-1 | 18.48 | 36.86 | 4.24 | 16.83 | 3.75 | 1.05 | 3.11 | 0.51 | 3.10 | 0.62 | 1.70 | 0.26 | 1.67 | 0.27 |
| 2B | 17.69 | 36.51 | 4.19 | 16.99 | 3.80 | 1.11 | 3.28 | 0.55 | 3.39 | 0.67 | 1.82 | 0.27 | 1.74 | 0.27 |

| | | | | | | | | | | | | | | |
|---|---|---|---|---|---|---|---|---|---|---|---|---|---|---|
| 2B (rerun) | 17.00 | 35.03 | 4.01 | 16.22 | 3.68 | 1.10 | 3.52 | 0.54 | 3.32 | 0.67 | 1.88 | 0.28 | 1.77 | 0.29 |
| 2B-2 | 15.37 | 30.37 | 3.65 | 14.93 | 3.47 | 1.05 | 3.07 | 0.50 | 2.99 | 0.60 | 1.67 | 0.24 | 1.56 | 0.24 |
| HELENA–HAYSTACK GREENSTONE; NORTHWEST CASCADE SYSTEM | | | | | | | | | | | | | | |
| 3E | 20.44 | 38.29 | 4.56 | 19.05 | 4.41 | 1.40 | 4.02 | 0.66 | 4.05 | 0.83 | 2.33 | 0.36 | 2.36 | 0.39 |
| EOCENE SILICIC VOLCANIC ROCKS | | | | | | | | | | | | | | |
| 36F | 22.61 | 45.99 | 5.80 | 25.98 | 7.22 | 1.60 | 7.87 | 1.42 | 8.95 | 1.84 | 5.02 | 0.73 | 4.50 | 0.71 |
| 53P | 17.11 | 35.48 | 4.37 | 19.11 | 4.14 | 1.32 | 3.37 | 0.48 | 2.67 | 0.51 | 1.30 | 0.18 | 1.07 | 0.16 |
| 36G | 40.12 | 76.27 | 8.73 | 36.01 | 8.98 | 1.13 | 8.39 | 1.44 | 8.84 | 1.86 | 5.23 | 0.79 | 4.99 | 0.78 |
| 40G | 34.20 | 66.39 | 7.68 | 31.32 | 7.96 | 1.03 | 8.03 | 1.41 | 8.66 | 1.77 | 4.85 | 0.71 | 4.51 | 0.72 |

### Trace elements continued (ppm)

| Sample | Ba | Th | Nb | Y | Hf | Ta | U | Pb | Rb | Cs | Sr | Sc | Zr |
|---|---|---|---|---|---|---|---|---|---|---|---|---|---|
| DACITE CLAST IN SAND AND GRAVEL OF MODERN SKAGIT RIVER ALLUVIUM | | | | | | | | | | | | | |
| SR | 498 | 5.15 | 4.86 | 15.54 | 3.49 | 0.39 | 1.79 | 9.80 | 38.2 | 2.41 | 447 | 12.2 | 124 |
| DACITE CLASTS IN EVERSON INTERSTADE RECESSIONAL OUTWASH | | | | | | | | | | | | | |
| 1D-1 | 536 | 5.96 | 4.88 | 16.40 | 3.92 | 0.43 | 1.92 | 11.17 | 40.4 | 2.57 | 515 | 11.9 | 138 |
| 2B | 562 | 5.99 | 4.73 | 17.44 | 4.02 | 0.45 | 1.73 | 10.80 | 37.3 | 2.42 | 536 | 13.8 | 142 |
| 2B (rerun) | 561 | 6.01 | 4.85 | 18.04 | 4.06 | 0.45 | 1.79 | 10.63 | 36.5 | 2.22 | 536 | 14.7 | 144 |
| 2B-2 | 417 | 4.94 | 4.13 | 15.74 | 3.47 | 0.36 | 1.54 | 8.47 | 31.1 | 1.60 | 535 | 14.4 | 126 |
| HELENA–HAYSTACK GREENSTONE; NORTHWEST CASCADE SYSTEM | | | | | | | | | | | | | |
| 3E | 377 | 3.38 | 5.80 | 21.69 | 3.45 | 0.38 | 0.88 | 2.54 | 44.0 | 1.43 | 47 | 10.8 | 123 |
| EOCENE SILICIC VOLCANIC ROCKS | | | | | | | | | | | | | |
| 36F | 588 | 4.87 | 12.66 | 48.17 | 5.72 | 0.89 | 1.60 | 8.72 | 58.3 | 4.04 | 195 | 29.9 | 207 |
| 53P | 1109 | 3.33 | 7.88 | 13.47 | 3.30 | 0.49 | 0.81 | 2.86 | 15.5 | 0.88 | 522 | 17.1 | 120 |
| 36G | 1035 | 12.27 | 14.47 | 47.26 | 7.91 | 1.07 | 3.97 | 22.28 | 114.3 | 2.36 | 50 | 7.5 | 250 |
| 40G | 1077 | 12.22 | 14.27 | 44.85 | 8.24 | 1.22 | 3.01 | 14.06 | 71.3 | 10.29 | 261 | 7.1 | 241 |

### Trace elements continued (ppm)

| Sample | Ni | Cr | Sc | V | Ba | Rb | Sr | Zr | Y | Nb | Ga | Zn | Pb | La | Ce | Th |
|---|---|---|---|---|---|---|---|---|---|---|---|---|---|---|---|---|
| DACITE CLAST IN SAND AND GRAVEL OF MODERN SKAGIT RIVER ALLUVIUM | | | | | | | | | | | | | | | | |
| SR | 16 | 15 | 13 | 76 | 513 | 42 | 446 | 141 | 15 | 4.7 | 15 | 56 | 9 | 22 | 35 | 6 |
| DACITE CLASTS IN EVERSON INTERSTADE RECESSIONAL OUTWASH | | | | | | | | | | | | | | | | |
| 1D-1 | 25 | 20 | 14 | 84 | 566 | 45 | 527 | 157 | 18 | 5.8 | 16 | 56 | 12 | 20 | 58 | 8 |
| 2B | 47 | 22 | 8 | 96 | 574 | 40 | 532 | 158 | 17 | 4.7 | 17 | 56 | 12 | 12 | 58 | 4 |
| 2B-2 | 21 | 30 | 14 | 115 | 426 | 32 | 537 | 139 | 17 | 4.6 | 16 | 58 | 8 | 11 | 29 | 1 |
| HELENA–HAYSTACK GREENSTONE; NORTHWEST CASCADE SYSTEM | | | | | | | | | | | | | | | | |
| 3E | 3 | 0 | 9 | 18 | 390 | 47 | 49 | 131 | 23 | 6.4 | 14 | 46 | 0 | 15 | 48 | 3 |
| EOCENE SILICIC VOLCANIC ROCKS | | | | | | | | | | | | | | | | |
| 36F | 2 | 4 | 28 | 48 | 612 | 57 | 93 | 211 | 48 | 13.0 | 25 | 128 | 5 | 17 | 48 | 6 |
| 36F (rerun) | 2 | 5 | 29 | 63 | 606 | 58 | 192 | 215 | 48 | 13.2 | 21 | 133 | 8 | 14 | 58 | 0 |
| 53P | 100 | 121 | 10 | 132 | 1172 | 16 | 513 | 130 | 13 | 6.9 | 17 | 85 | 5 | 4 | 29 | 4 |
| 36G | 6 | 0 | 7 | 9 | 1092 | 115 | 46 | 244 | 47 | 14.2 | 16 | 62 | 20 | 33 | 84 | 11 |
| 40G | 5 | 0 | 9 | 3 | 1091 | 77 | 272 | 256 | 46 | 14.3 | 22 | 122 | 16 | 26 | 59 | 11 |

# Appendix 4. Glacier Peak volcanic detritus in recessional glacial outwash—Petrologic, petrographic, and geochemical evidence

Our geochemical (Appendix 3), sand point-count (Appendix 2), dacite clast petrographic information, and field relations indicate that outwash containing a significant Glacier Peak dacite detritus was deposited concurrently with glaciomarine drift in the southern Conway quadrangle. (Figure 3 shows the proximity of distal White Chuck assemblage lahar and volcanic alluvium deposits to the study area.) That is, the amount and character of these dacite clasts indicate that the late glacial (~11,250–12,500 yr B.P.) White Chuck assemblage of Beget (1981, 1982) was incorporated into late glacial outwash and deposited near the intersection of the Stillaguamish River and the late-glacial Puget Sound. That the dacite is of Glacier Peak origin is best evidenced by the geochemistry of the clasts (Appendix 3). These clasts are geochemically very similar to Glacier Peak dacite found elsewhere (Dragovich and others, 2000a, unpub. data). Also, the petrography of two gravel-size dacite clasts (samples 1D-1 and 2B-1, Fig. 4 and Appendix 3, Table B) indicates that the dacite is of homogeneous composition. These augite-hypersthene-hornblende-phyric dacite clasts are similar in appearance to the Glacier Peak microlitic volcanic clasts in the sand fraction described below. Two point-counted samples of outwash sand (samples 9R and 1D, Fig. 4 and Appendix 2, Table B) indicate two significantly different provenances for the outwash; far-traveled northern detritus (source 1), and local "Stillaguamish" (source 2). (Figure 3 shows source 2 as a large alluvial fan–deltaic system.) Sample 9R is typical Everson source 1 outwash and contains mostly monocrystalline quartz (17%), quartz mica tectonite, polycrystalline quartz and chert (21%), plagioclase (12%), sedimentary, metamorphic, and quartzo-feldspathic lithic clasts (29%). This sample appears to have a polymictic provenance with a combination of exotic northern detritus (for example, Coast Mountains granitic clasts) mixed with local source detritus (for example, greenstone, serpentinite, phyllite) and contains only 3 percent microlitic volcanic fragments. Conversely, the fluvial recessional outwash overlain by a thin mantle of glaciomarine drift well exposed in the CM Trucking sand and gravel quarry (site 1D, Fig. 4) represents source 2. The sand is significantly more volcanic-lithic and contains mostly monocrystalline quartz (20%; including significant volcanic quartz), quartz mica tectonite, polycrystalline quartz and chert (9%), plagioclase (22%), as well sedimentary, metamorphic, and quartzo-feldspathic lithic clasts (21%). This outwash contains semivesicular dacite clasts that have a petrographic signature similar to Glacier Peak dacitic clasts studied elsewhere. Most importantly, this sample contains 13 percent microlitic hypersthene-, hornblende-, and augite-phyric volcanic fragments and 2 percent detrital hypersthene and appears to have a partial but distinct Glacier Peak volcanic provenance. Also, the occurrence of augite as a Fe-Mg phenocryst in the microlitic volcanic clasts is consistent with the composition of the dacitic lithic clasts of the late-glacial White Chuck volcanic assemblage (Beget 1981, 1982). Additionally, some of the dacite clasts are petrologically and texturally very similar to the White Chuck tuff (Jerry Ladd, Western Washington Univ., oral commun., 2002). This tuff is found in the uppermost part of the White Chuck assemblage and is texturally distinctive. The occurrence of these distinctive Glacier Peak clasts in Everson outwash has important paleogeographic inferences for the Everson deposits. For example, the occurrence of Glacier Peak clasts in outwash argues for a western Stillaguamish River (ice-free?) source for some of the Everson outwash deposition concurrent with glaciomarine deposition.